A STUDY OF PHASE TRANSITIONS IN CRYSTALLINE SOLIDS

DISSERTATION

SUBMITTED IN PARTIAL FULFILMENT OF THE REQUIREMENTS
FOR THE AWARD OF THE DEGREE OF

Master of Philosophy

IN

PHYSICS

BY

ABDUS SATTAR

DEPARTMENT OF PHYSICS
ALIGARH MUSLIM UNIVERSITY
ALIGARH (INDIA)

1992

To My Parents

DEPARTMENT OF PHYSICS
ALIGARH MUSLIM UNIVERSITY
ALIGARH U. P. (INDIA)
Tele No. : 4568

CERTIFICATE

Certified that Mr. Abdus Sattar has carried out the work on **"A STUDY OF PHASE TRANSITIONS IN CRYSTALLINE SOLIDS"** under my supervision and this work is suitable for submission for the award of the degree of Master of Philosophy.

25.5.92

(Dr. J.P. SRIVASTAVA)

ACKNOWLEDGEMENTS

I am greatly pleased to express my deepest sense of gratitude to my supervisor **Dr. J.P. Srivastava** for his able guidance, invaluable encouragement and keen interest during the course of my work. I am also deeply indebted to him for carefully reading the manuscript, valuable criticism and making numerous improvements in the presented work.

I am very thankful to **Prof. B.N. Khanna**, Chairman, Department of Physics, A.M.U., Aligarh for providing me the work facilities in the department and taking interest in the progress of my work.

I am extremely grateful to **Prof. A.L. Verma**, Department of Physics, N.E.H.U., Shillong for allowing me to work in his laboratory and extending valuable guidance. I am indebted to **Prof. Kamal Kumar**, Department of Physics, N.E.H.U., Shillong for his tender and helpful attitude towards me during my stay at Shillong. My special thanks are due to **Mr. A.K. Rathore**, Technical Assistant, Laser Raman Spectroscopy Lab., N.E.H.U., Shillong for his help in recording Raman spectra.

I am grateful to **Dr. Mushtaq Ahmad** and **Mr. M. Abul Hossain**, Department of Physics, A.M.U., Aligarh for their constant help, encouragement and suggestions. I am also thankful to **Dr. S.A. Ali**, Department of Geology, A.M.U., Aligarh who was always with me with his keen interest, timely advice and help.

I gratefully acknowledge U.G.C., India for financial support during the period of my research work. The technical assistance from the staff of the Department of Physics, A.M.U., Aligarh is also appreciated.

I am particularly thankful to my respected **parents, brothers, sisters** and other members of my family for their tremendous patience, constant encouragement and moral support throughout the course of work. I also tender thanks to respected **Mr. A.K.M. Minhazzudin** for motivating me to concentrate on my research work.

Finally, I feel sincerely indebted to all my well wishers and friends, specially - **Mrs. Nazma Akhter Banu, Mr. Siraj Uddin Ahmed, Mr. Badruddoza, Mr. Md. Niamat Ali, Mr. G.M. Khan, Mr. A. Hassan, Mr. Hafizur Rahaman, Mr. N.C. Biswas** for their close association and encouragement. I would also like to thank **Mr. Shujaat Ali** for taking extra care in typing this dissertation.

26.5.92

(ABDUS SATTAR)

CONTENTS

		Page
GENERAL INTRODUCTION.		1
REFERENCES		7
CHAPTER - I		
THEORETICAL BACKGROUND		
1.1	Introduction	8
1.2	Phase Transition	9
	1.2.1 Classification	9
1.3	Structural Phase Transition	11
1.4	Martensitic Phase Transition	18
1.5	Response Function and Order Parameter	20
1.6	Landau Theory of Phase Transition	20
1.7	Soft Mode	23
	1.7.1 Coupled Soft Mode	24
1.8	Hard Mode	25
1.9	Critical Phenomenon	25
1.10	Dynamics of the Crystal	26
1.11	Classification of Phonon	29
	1.11.1 Unit Cell Approach	30
	1.11.2 Site Symmetry Approximation - Correlation Method	33
1.12	Internal Modes of Vibration of Molecular groups of the Crystal under study	36

1.13	Anharmonicity and Interaction of Vibrations		37
1.14	IR Spectroscopy		40
	1.14.1	General	40
	1.14.2	Selection Rule	45
	1.14.3	Analysis of IR Spectra	46
1.15	Raman Scattering		47
	1.15.1	General	47
	1.15.2	Selection Rule for Raman Scattering	53
	1.15.3	Analysis of Raman Spectra	54
REFERENCES			55

CHAPTER - II

EXPERIMENTAL TECHNIQUES

2.1	Introduction		60
2.2	Preparation and Growth of Crystals		60
2.3	Experimental set up for Raman Spectra measurement		60
	2.3.1	Source	62
	2.3.2	Spex Ramalog System	62
	2.3.3	Scan of Raman Spectra	65
	2.3.4	Measurement of Raman Spectra at different temperature	67
	2.3.5	Factor affecting the intensity of the recorded spectrum	67
	2.3.6	Calibration of the spectrometer	70
	2.3.7	Precautions	71

2.4 IR Instrument 71

2.4.1 Measurement of IR Spectra 72

2.4.2 The Nujol-Mull Technique 74

2.4.3 The Pressed disc (Pellet) Technique 75

REFERENCES 76

CHAPTER - III

VIBRATIONAL SPECTRA AND PHASE TRANSITION

3.1 Introduction 77

3.2 Crystal Structure 82

3.3 Factor Group Analysis 84

3.4 Results and Discussions 89

3.4.1 Vibrational Spectra and bands assignment at room temperature 89

3.4.2 Temperature dependent Raman Spectra and Phase Transition 97

3.5 Conclusions 104

REFERENCES 105

#####

GENERAL INTRODUCTION

Smoothness and continuity are desired in many branches of physics where questions of mathematical rigor are given secondary importance. Nowadays, materials are used for various purposes. So the studies of the properties of materials are very useful. Out of these properties, the study of phase transition has attracted the attention of scientists for so many years. There has been a vigorous research activity in the area of phase transition during the recent past. But many of these studies were short-lived and have become obsolete with the new developments.

A material may exist in several phases of structure. A material may change from one phase to the other under the influence of some perturbation like temperature, pressure, electric or magnetic field etc.[1]. Knowledge of initial and final structure is mostly required to understand what happens when a transformation takes place[2]. However, the questions like how and why the transition occurs are yet to be answered. From wealth of available information, it is possible to classify and identify phase transformations in solid state physics. Some of the physical properties may change during phase transitions. Explanations to their observed behaviour in many cases are conflicting. Phase

transitions are essentially co-operative phenomena in which many particles must interact with each other at the same time[3]. It was recognized at the early stage that the phase transitions are associated with the interactions between the macroscopic constituents of the system[3]. But an exact treatment by means of statistical mechanics appeared preventively difficult in this regard. During the latter part of 19th and the earlier part of 20th century, phenomenological explanations were schemed which seem to account sufficiently for the discontinuity and provide insight into their detailed characteristics[3]. The crowning achievement in the phase transition is the Onsager's two dimensional Ising-model[4] in which he succeeded in carrying out an exact statistical mechanical calculation for simple interacting atomic model in 1944 and it started the modern era in phase transition. A simple physical picture of the dynamical mechanism of a phase transition is developed in mean field approximation[5]. In recent years, increasing number of experimental and theoretical studies have been reported on structural phase transition (SPT) and soft modes which deserve our attention[6]. During 1960's considerable progress was made towards the greater understanding of phase transition and critical phenomena[3]. However, the understanding of the dynamics through microscopic soft mode theory or critical phenomena is quite incomplete. Several useful reviews have been published in this field[3,6-9].

Over the last decade, the use of various complementary experimental techniques with their specific merits are in our hand. Different spectroscopic techniques have been employed, including infrared (IR) reflectively, inelastic light and neutron scattering, EPR, NQR, X-ray and ultrasonic analyses[8]. The only pre-war spectroscopic investigation of a solid state structural phase transition was that of Raman and Nedungadi in quartz[10]. Very few experimentalists have covered scattering technique as well as magnetic resonance methods with a comparable degree of ability, although useful contributions to the field have been obtained by both the techniques. Now, the use of laser led to a renaissance in light scattering. The vibrational spectroscopic studies supply deeper insight into the microscopic origin of structural phase transitions[9]. The study of vibrational properties help in understanding the dynamics of orientation of molecular groups and atoms in crystals. It also provides information about molecular structure and the nature of force that bind the various atomic and molecular units inside a crystal.. The Raman and IR absorption spectroscopic measurements are being used to study the vibrational properties. The effect of crystalline field on vibrations of crystals can be comprehended by these techniques through polarization measurements. In Raman technique, the light is scattered due to the fluctuation in the dielectric tensor of the material. Near phase transitions the

fluctuations of some of the physical quantities coupled to the dielectric tensor are enhanced and affect the integrated scattered intensity, peak frequency and the line width of the spectral power density[9]. Thus the measurement of these quantities yield information about the structure and dynamics of the solid undergoing the phase transition. This makes the Raman scattering a valuable tool for the study of structural phase transition. The entire vibrational spectrum upto 4000 cm^{-1} can also be traced out in a single run of the spectrum in Raman scattering whereas IR technique requires separate measurements for the far-infrared (FIR) and near-infrared (NIR) spectral regions.

In order to understand common features of phase transitions in crystals we have selected $(NH_4)_3\ H(SO_4)_2$ which is known to undergo a numerous phase transformations with the change of temperature. We have employed IR and Raman spectroscopic techniques for investigations. This compound belongs to a double salts group of the general formula A_3HB_2, where A is an alkali metal or NH_4^+ ion and B represents SO_4^{2-} or SeO_4^{2-} ion. This system is interesting since it contains very strong and unusual O-H···O hydrogen bonds linking SO_4^{2-} ions into a $(SO_4HSO_4)^{3-}$ dimer[11]. At atmospheric pressure and above liquid nitrogen temperature this crystal exhibits five successive phase transition[12].

It also shows ferro-electricity below 46K[13]. The deuterium substitution or the application of pressure also stabilizes a ferro-electric phase in this crystal[14,15]. The present dissertation consists of three chapters.

In Chapter-I, general theoretical aspects of structural phase transitions are described. The group theoretical methods for the classificaion of normal modes, classification of internal modes of vibration of molecular groups present in the crystal, anharmonicity and interaction of vibrations, theory of IR and Raman scattering and their selection rules are also included in this chapter as this knowledge is a pre-requisite to the understanding of phase transformations.

Chapter-II deals with details on crystal growing procedure, verification of crystal structure alongwith a brief description of the principle of working of equipments used for our studies.

Chapter III delineates our experimental observations i.e. the vibrational analysis of spectra and the characteristics of the observed structural phase transitions as permissible under the known crystalline symmetry. We have concentrated on transitions at phase III $\xrightarrow{140\ K}$ phase IV and phase IV $\xrightarrow{133\ K}$ phase V. The phase

transitions are characterized by the temperature dependence of HSO_4^- symmetric stretching mode ν_1^s which is found to be the most thermosensitive. The observed continuous change in peak intensity and FWHM of HSO_4^- symmetric stretching mode with temperature around 140 K and abrupt change in peak intensity and FWHM around 133 K are typical features associated with phase transitions of the second order and first order type respectively. Narrowing of the FWHM of HSO_4^- symmetric stretching mode at lower temperatures and downward shift of N-H stretching mode with temperature lowering suggest that reorientational motion of sulphate and ammonium ions are responsible for these transitions. This also suggests that the strength of hydrogen bonding also increases with decreasing temperature.

REFERENCES:

1. Bruce A.D. and Cowlay R.A. "Structural Phase Transitions" Tayler and Francis Ltd., London (1981).
2. Frazer B.C. in "Structural Phase Transitions and Soft Modes" ed. by Emil. J. Samuelsen, Eigil Andersen and Jens Feder, Universitetsforlaget, Oslo, (1971).
3. Domb C. and Green M.S. "Phase Transitions and Critical Phenomena" Academic Press, London (1972).
4. Onsager L., Phys. Rev. **65** 117 (1944).
5. Thomas H. in "Structural Phase Transitions and Soft Modes" ed. by Emil J. Samuelsen, Eigil Andersen and Jens Feder, Universitetsforlaget, Oslo (1971).
6. Samuelsen J.E., Andersen E. and Feder J. "Structural Phase Transitions and soft modes" Universitetsforlaget, Oslo (1971).
7. Müller K.A. and Thomas H. "Structural Phase Transitions" Springer-Verlag, Berlin (1981).
8. Scott J.F., Rev. Mod. Phys. **46** 83 (1974).
9. Iqbal Z. and Owens F.J. "Vibrational Spectroscopy of Phase Transitions" Academic Press, INC. Orlando (1984).
10. Raman C.V. and Nedungadi T.M.K., Nature **145** 147 (1940).
11. Damak M., Kamoun M., Daoud A., Romain J., Lautie A. and Novak A., J. Mol. Struc. **130** 245 (1985).
12. Gesi K., Phys. Status Solidi **a33** 479 (1976).
13. Gesi K., Japan J. Appl. Phys. **19** 1051 (1980).
14. Gesi K., J. Phys. Soc. Jpn. **41** 1437 (1976).
    ibid. **43** 1941 (1977).
15. Osaka T., Makita Y. and Gesi K., J. Phys. Soc. Japan **43** 933 (1977).

CHAPTER - I

THEORETICAL BACKGROUND

THEORETICAL BACKGROUND

1.1 INTRODUCTION

A material may exist in several phases. The term phase represents structural state of the material with characteristic uniform physical and chemical properties. The material changes from one phase to the other under the influence of some perturbation like the change of temperature or application of fields including pressure[1]. The phase changes, popularly known as phase transitions, control the properties of materials to a large extent sometimes. Therefore, the study of phase transitions is vital for various applications in material science. The subject has gained growing interest in the field of solid state Physics, Chemistry, Biology and Engineering. The knowledge of structural and crystallographic characteristics of distinct typical transformations is a pre-requisite for understanding the properties of materials. In the following section we discuss various types of phase transitions. The theoretical aspect of structural phase transitions has been, however, taken up in detail. The properties of solid depend on phase transition can be studied by spectroscopic methods[2]. Scott[3], Steigmur[4], Nakamure[5] and Flury[6] reviewed the structural phase transition (SPT) by Raman scattering studies.

We will first give a brief account of phase transitions and their classification in current interest. Then we will discuss basic concepts related to structural phase transitions, including some of the recent ideas in brief. Normal mode classification in crystals, group theoretical methods, classification of normal modes of vibration of the crystal under study and a brief discussion of the theory of Infrared and Raman scattering are given later.

1.2 PHASE TRANSITION

Due to the application of an external agent, like temperature, pressure, magnetic field or electric field, strain etc., a substance changes state. This change of state is called **phase transition**[1]. On account of phase transition the overall symmetry of the crystals may not change. The macroscopic and microscopic properties of the system depend on these transitions. Their studies are important for applications of materials, like use of ferroelectrics as piezoelectric components and pyroelectric detectors, computer core storage in magnetic ferrite rings, liquid crystals display etc.[1,7,8].

1.2.1 Classification

There are many classes of phase transitions on the basis

of different criteria. In one of the general ways phase transitions may be classified as follows:

(a) Reversible and Irreversible phase Transition: The transition which the system returns to its original phase after withdrawal of the external agency, responsible for the transition, is called **reversible phase transition.** But in **irreversible transition,** the system does not return to its original phase. The change of graphite to diamond is an example of irreversible phase transition.

(b) First Order and Second Order Phase Transition: According to the nature of change of properties, a phase transition is classified as first order or second order type. When the physical and chemical properties of the system change quickly i.e. discontinuously then it is called a **first order transition.** In this transition there are no predictable symmetry but two states are in equillibrium. If the change of some properties of the state is very slow i.e. continuous, then it is known as a **second order transition**[9]. It is also called λ -point transition because of the nature of the change. Here two phases have the same symmetry at transition point. Gibbs has given the thermodynamical theory of the first kind and Ehrenfest has further extended it to the second kind by considering Clausius-Clapeyron relation[10,11]. Landau also clarified more general theory on λ -transition[9]. Near second order phase

transition the crystal becomes soft with respect to the order parameter[12]. Considering this soft mode criterion, Thomas discussed the dynamics of second order transition[13].

(c) Bürger Classification: From crystallographic point of view, Bürger[14] have been classified the phase transitions mainly as Displacive, Reconstructive and Martensitic. However, in broad sense we classify them as structural and martensitic phase transition. With reference to the work reported in this dissertation, the structural phase transitions require a proper introduction here and this is presented in the following text.

1.3 STRUCTURAL PHASE TRANSITION

Structural phase transition (SPT) is now a current topic in solid state physics. It can be discussed from different points of view[12,15]. Generally, the structure change in the phase transition occurs in two distinct ways. In one case a new lattice is formed through rearrangement of atoms in the system, such a transition is called **Reconstructive Phase Transition.** In this transition there are no symmetry relations, therefore, it is first order in nature. It is very slow process. The change of silicon from amorphous to microcrystalline is the best example of this type of transition. In

the other case system as a whole does not change but periodic lattice is distorted slightly through (i) a small displacement of the lattice positions of atoms or molecular groups and (ii) the ordering of atoms or molecular units. This phase transition is second order type.

In terms of order parameter, structural phase transitions are further classified as (i) **Displacive,** (ii) **Order-disorder** and (iii) **Electronic.** The displacive and order-disorder type transitions are described in terms of atomic order parameter, whereas electron-lattice coupled order parameter is involved in electronic type transition. The distinction between order-disorder and displacive transitions can be made by considering single-cell potential, which may be written for one spatial coordinate Q with anharmonic potential as

$$V(Q) = aQ^2 + bQ^4 \qquad (1.1)$$

Here 'a' and 'b' are constants satisfying $a < 0$, $b > 0$. The schematic diagram of this type of single cell potential is shown in Fig. 1.1[12]. Equation (1.1) represents a double-well potential where there are two minima and a maximum with energy difference ΔE. If $\Delta E >> kTc$, the transition occurs due to dynamic ordering at one site or orientation i.e. at one of the potential minima along Q where Tc

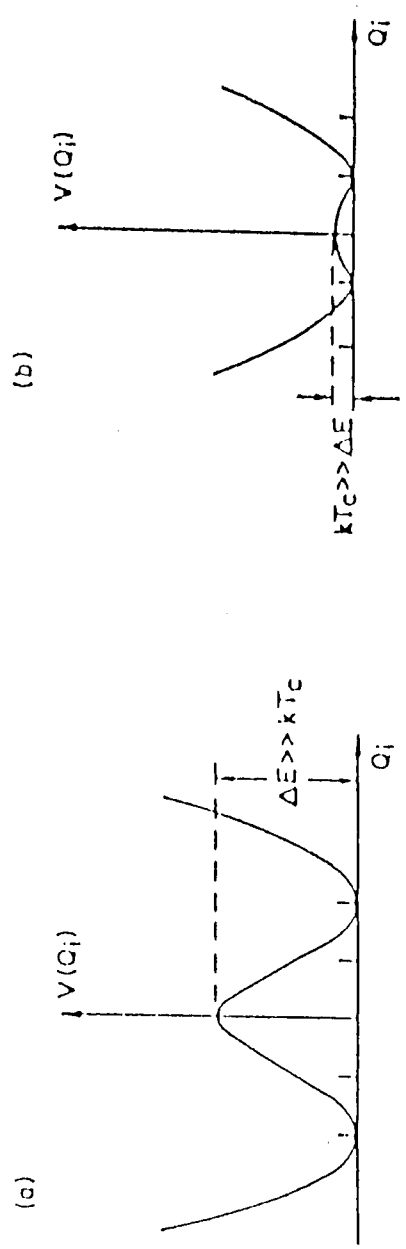

Fig. 1.1. Single cell potentials in (a) order-disorder (b) displacive SPT system

is the transition temperature and k is Boltzman constant. Again this order disorder phase transition is of two types, one due to **ordering of H-atom** which is observed in hydrogen bonded ferroelectrics such as KDP. (Potasium dihydrogen phosphate) and the other one due to **ordering of molecular or molecular-ionic orientation.** It occurs in sodium nitrite ($NaNO_2$).

When depth $\Delta E << kTc$, a continuous cooperative displacement of atoms along Q occurs below Tc with temperature. It is called a **Displacive SPT.** There are three types of displacive SPTs:

i. **Ferro-distortive:** It involves the displacement caused by a long wave length ($k \sim o$) optic phonon without changing number of formula units per unit cell. This transition occurs in $BaTiO_3$.

ii. **Antiferro-distortive:** It is related with displacement caused by a short wave length optic phonon. It is also called **zone boundary transition.** In this transition the number of formula units in unit cell changes by an even integral multiple. The example for this transition is $SrTiO_3$.

iii. **Thermo-elastic:** It concerns displacements corresponds to long wave length acoustic mode, that is represented by a

macroscopic strain. This transition is found in TeO_2. The ferrodistortive and thermo-elastic transitions can give rise to ferroelectric phases. Thermo-elastic transitions are referred to as **ferro-elastic.**

However, the dynamical behaviour of that two distortive SPTs are different. There are many order-disorder systems. The excitation spectrum of magnetic systems shows relaxation character above Tc and centered around zero frequency. A finite frequency mode is observed below Tc. In displacive transition, finite frequency mode also exists above Tc which tends to freeze out on approaching Tc from above. It is shown very clearly by soft mode theory. In some molecular or molecular-ionic crystal order-disorder transition is explained through displacive transition, like KCN[16-18] which is orientationally disordered in high temperature but ordering is explained through displacive and rotational-translation coupling. In this type of crystals the displacive and order-disorder transitions are distinguished clearly by considering molecular-ionic flipping rate[16].

Two categories are observed in **Electronic transition.** One is called **Jahn-Teller (JT),** where the coupling of electronic and acoustic degrees of freedom take place. It also interacts with a localized electronic level (e.g. $TbVO_4$) or with a delocalized level

(e.g. Nb_3Sn). The first one is known as **Cooperative Jahn-Teller (CJT)** and second one as **Band Jahn-Teller (Band JT).** First Elliott et al[19] and then Pytte[20] supplemented the theory of CJT in terms of electronphonon interaction. Another class of electronic transition is **charge density wave (CDW)** which is observed in low dimensional structure metallic systems. Here conduction electronic density shows a periodic nonuniformity. Interaction between electron and lattice of the one dimensional system opens a gap at the Fermi wave vector $\mathbf{k}_F$ and gives an insulating state[21] whereas in three dimensional metal Kohn anamalies occur is phonon spectrum for wave vector $2\mathbf{k}_F$.

There is also **improper ferroelectric SPT,** in low temperature phase. Macroscopic polarization is induced through different symmetry order parameter coupling (higher order). It involves mainly a degenerate (high temperature phase) order parameter with displacements corresponding to a zone boundary vibrational mode. Gadolinium molybdate $Gd_2(MoO_4)_3$ is an well studied example of this class[22,23].

Therefore from above discussion we can classify SPTs as follows:

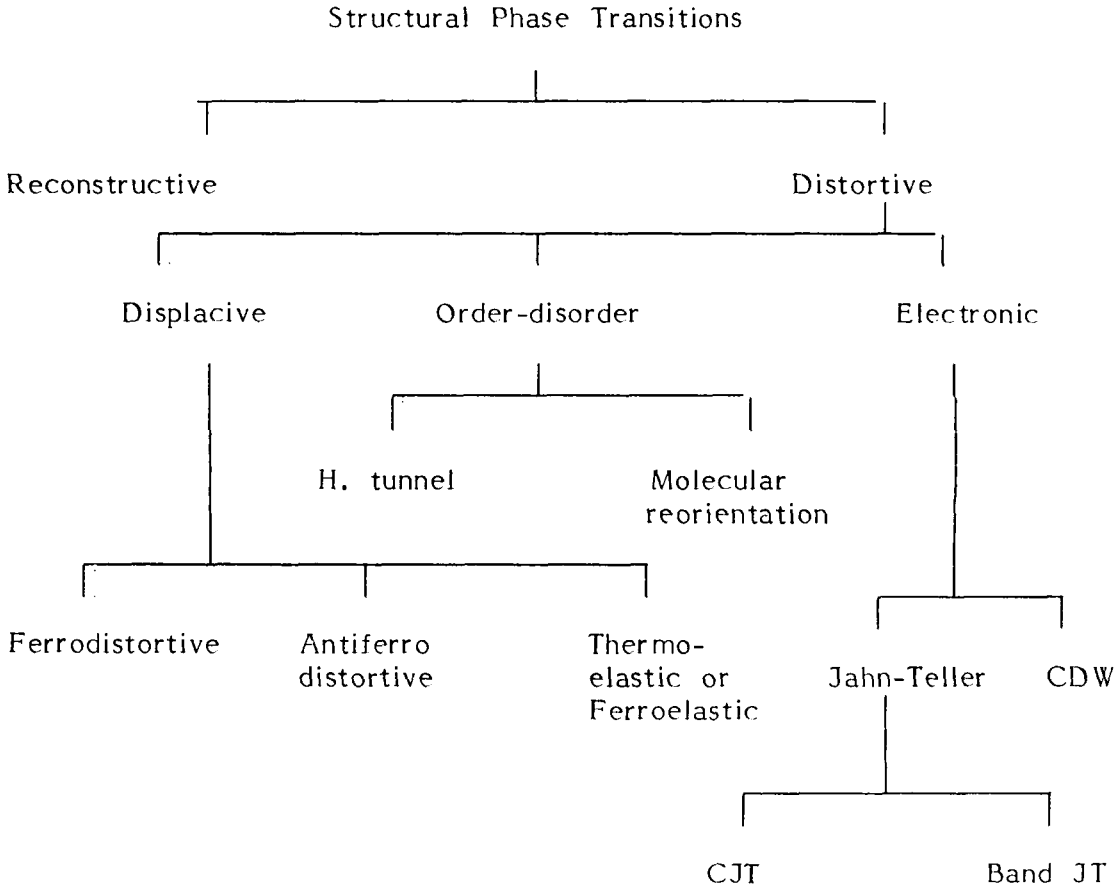

Another transition called **Incommensurate Transition** has attracted sufficient attention and it is not yet completely understood[24]. A numerous examples have become known of compounds having in certain temperature interval a structure without any space group symmetry, whereas outside that interval the structure is crystalline. The non-crystalline structure is not amorphous but is well ordered and may be described as a periodic distortion not fitting with the crystal periodicity[7]. In this transition unit cell volumes at the parent or prototypic phase

(high-symmetry phase) and lower symmetry phase are related by multiple of an irrational number whereas if the number is rational, it is called **Commensurate Transition,** such as ferro and antiferro-distortive phases. The incommensurate transition is well known in magnetism. The distortion arising in incommensurate transition, is shown in figure 1.2[25]. The order parameter of the eigenvector of soft mode $\delta \mathbf{u}$ depends on both amplitude and phase[26]. For incommensurate phase transition

$$q_j = 2\pi (1-\delta)/na, \qquad (1.2)$$

where 'a' is the lattice constant of parent phases, 'n' is an integer and 'δ' is an irrational number; small compared to unity. In this phase transition amplitude $|\delta \mathbf{u}|$ changes uniformly like commensurate, and phases of $\delta \mathbf{u}$ are shifted uniformly. K_2SeO_4 is the more well defined example of incommensurate phase transition[25].

1.4 MARTENSITIC PHASE TRANSITION

Martensitic transition is a diffusionless i.e. crystal lattice does not interchange places and is related only by shear deformation in two phases. Crussard[27] discussed this type of transition with the help of Nucleation theory. Most of the alloys shows this phase transition e.g. $Au_x\ Cu_{y-x}\ Zn_{1-y}$ etc.

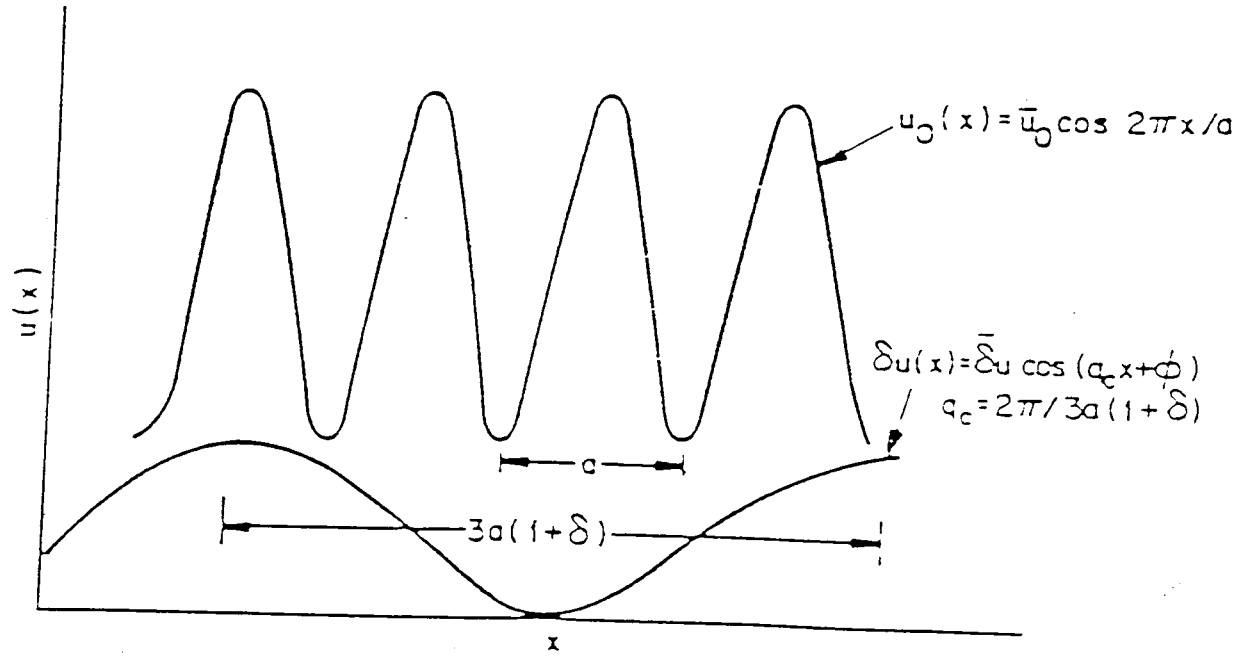

Fig. 1.2. Schematic representation of an incommensurate phase transition. The static particle displacements in the parent phase (u_0) are shown, together with the incommensurate distortion δu. The incommensurate structure is determined by the sum $u_0(X) + \delta u(X)$.

1.5 RESPONSE FUNCTION AND ORDER PARAMETER[12]

Due to phase transition, some parameters called **Response Functions** are changed. These are mainly thermodynamical quantities, like Gibb's free energy. From the gradient of that function we can defined the order of transition. There is another observable quantitative property of the system which responds to the external agent, like thermal gradient etc. and vanishes above the transition temperature. It is named as order parameter (η). Its behaviour is significant to the discussion on phase transitions.

In SPTs η measures the change of the atomic geometry in the low temperature phase from parent phase. There are large number of order parameters in the SPTs, like magnetisation (M), polarization (P) etc. The order parameter can be calculated experimentally only for the second order transition.

1.6 LANDAU THEORY OF PHASE TRANSITION

The light scattering studies are the conspicuous process to investigate the symmetry aspects of the system. For this interest Landau developed a symmetry based theory on second order phase transition[9,28]. It is also valid for weak first order transition. Landau imposed some assumption in his theory as follows:

i. The ion density or electron density $\rho(\mathbf{r})$ giving a new distribution

$$\rho(\mathbf{r}) = \rho_0(\mathbf{r}) + \Delta\rho(\mathbf{r}), \tag{1.3}$$

where $\rho_0(\mathbf{r})$ is parent phase electron density which is invariant in higher symmetry and $\Delta\rho(\mathbf{r})$ small change in the lower symmetry. Landau postulated that symmetry group of $\rho(\mathbf{r})$ must be a subgroup of the symmetry group of $\rho_0(\mathbf{r})$.

ii. In terms of n-th irreducible representation basis $\phi_{n,i}(\mathbf{r})$ (i-dimensional) of the symmetry group of $\rho_0(\mathbf{r})$, we can write

$$\nabla\rho(\mathbf{r}) = \sum_{n,i} C_{n,i}\Phi_{n,i}(\mathbf{r}) \tag{1.4}$$

where $C_{n,i}$ are the coefficient term. Landau considered that in continuous phase, the different irreducible representation set at same temperature come only by accident. So, second order transition be adequate for single irreducible representation and $\Delta\rho(\mathbf{r})$ can be written as:

$$\nabla\rho(\mathbf{r}) = \sum_{i} C_i\Phi_i(\mathbf{r}) \tag{1.5}$$

where C_i is the coefficient proportional to order parameter.

iii. Near transition point, the free energy F of a crystal is written interms of order parameter as,

$$F = F_o + \alpha\eta + \beta\eta^2 + \gamma\eta^3 + \delta\eta^4 + \cdots \quad (1.6)$$

where coefficients α, β, γ, δ ---- are functions of pressure and temperature. Imposing equillibrium condition

$$\frac{\delta F}{\delta \eta} = 0 \text{ and } \frac{\delta^2 F}{\delta \eta^2}_{\eta=\eta_0} > 0 \quad (1.7)$$

we find out $\beta = 0$ at transition point and α also be zero for $\eta = 0$ and $\eta \neq 0$ have different symmetry. Landau assumed that for the second order transition the coefficient of cubic term must be zero. The other condition is that $\delta > 0$, otherwise the transition will be first order type.

iv. Only wave vector K, which is simply a fraction of reciprocal lattice vector of prototypic phase, and allowed in second order transition represents the basis function in the

following form:

$$\Phi_i(\mathbf{r}) = u_{i,k}(\mathbf{r})\, e^{i\mathbf{k}\cdot\mathbf{r}} \tag{1.8}$$

1.7 SOFT MODE

From Landau's thermodynamic stability condition, we can write

$$\eta = \eta_o \mid T-T_c \mid^{\frac{1}{2}} \tag{1.9}$$

and $$\omega = \omega_o \mid T-T_c \mid^{\frac{1}{2}} \tag{1.10}$$

These equations tell us that there is a mode of vibration which goes to zero frequency at T_c. This mode is called **Soft Mode.** Actually energy falls at transition point due to interaction between soft mode and acoustic mode[28]. This soft mode in Raman spectroscopy was first described by Raman and Nedungadi[29] in quartz. From dynamical point of view this soft mode concept was invoked by Cochran[30] and later by Anderson[31]. Anharmonic contribution is needed for discussing clearly the experimental results[32,33]. Using Lyddane-Sachs-Teller relation, Frohlich[34] concluded that in ferroelectric SPTs, only transverse optic phonon is leading the phase transition. In displacive transition the

anharmonic contribution is small but it is large for order-disorder transition[15].

1.7.1 Coupled Soft Mode

Low frequency response function has two components above T_c, one due to soft phonon and other called **Central Peak Component**[15]. It is a quasi-elastic component, relaxation type centred at $\omega = 0$, whose intensity quickly grows as $T \longrightarrow T_c$ and completely dominate the scattering close to T_c. It was explained by considering the theoretical model like, anharmonic perturbation theory, impurity and intrinsic phenomenon like cluster formation. The central peak component is observed in wide variety of SPTs and also in materials ranging from insulator to metal . Its contributions are very small but measurable width in wave vector.

A rich variety of SPTs are known to occur in a large number of materials due to the coupling between primary and secondary order parameters. For examples, we take anti-ferrodistortive improper SPTs (e.g. in $Gd_2 (MoO_4)_3$) which is one of the three kinds of coupled systems detected and investigated. In this case the primary order parameter, corresponding to a mode at a zone boundary point, induces a net spontaneous polarization, which is the **secondary order parameter**[15].

1.8 HARD MODE

Some modes other than soft mode, responsible for phase transition are called **Hard Modes**[35]. They consist of either activation of silent modes or the splitting of degenerate modes or of both below the transition temperature. The changes of mode frequency and strength can be expressed in terms of spontaneous value of the order parameter η [36]. This theory is applied to eighteen SPTs for which experimental data are known[37]. Infrared activation of hard modes is best understood in quartz[38].

1.9 CRITICAL PHENOMENON

Critical point concept can be used for characterization of the phase transition in many physical systems. It is normally defined in terms of a temperature or pressure parameter. Actually the behaviour near the critical point is described by critical exponent, which states clearly the temperature dependence of the macroscopic properties, like order parameter (η), susceptibility (χ) and a correlation length (ξ)[15]. **Critical exponent** is defined by some power of the reduced temperature. This theory is valid only for second order transition. The value of critical exponents is determined by microscopic model applied for different models, the value of critical exponent is given in the table 1.1[15].

Table 1.1

Properties	Exponent	Any d MFT	(Lattice d = 3) Ising	XY	Heisenberg
Order parameter	β	.5	.325	.346	.365
Susceptibility	γ	1	1.24	1.316	1.387
Specific heat	α	0	.110	-0.007	-0.115
Correlation length	ν	.5	.63	.669	.705

The value of critical exponents depends on range of the force, the lattice dimensionality (d) and number of spin components. The value ν is same for different model, so it is called universality class.

1.10 DYNAMICS OF THE CRYSTAL

To know the details of vibrational spectroscopy, the idea of lattice dynamics is necessary. The question of vibration in lattice was raised by Taylor, Euler, Fourier and Lagrange. Later, considering one dimensional model of NaCl, Bron discussed the dynamics of crystal lattice[39].

A crystal may be considered as a mechanical system of nN particles, where N is number of unit cell and n is the number of particles per unit cell. This system has 3nN degrees of freedom where 3nN-3 are linearly independent normal modes of oscillation of

of the crystal and three are pure translation[40]. A normal mode has the properties such as, (a) atom of the system oscillates about its equilibrium position with simple harmonic motion with the same frequency and phase, and (b) the relative velocity and amplitude of an individual atom depends on its mass. It is also related linearly to the internal coordinate of the system[39]. The normal mode frequencies are to be found as the 3n roots of the secular equation, involving the wave vector. It may take N values. Three of these roots tend to zero as the wave vector approach zero and are named as the **acoustic branches.** The remaining 3n-3 branches are designated as the **optical branches** and take finite limits as the wave vector vanishes. These branches can also be classified as **longitudinal** and **transverse branches**[41]. These constitute the fundamental vibrational spectrum of the crystal. The frequency distribution in an individual branch is obtained by calculating the number of roots in each small interval of frequencies.

In normal coordinate system, the nature of motion is so controlled that no net translation or rotation of the system as a whole takes place[42]. Each mode of vibration follows the quantization rule and the term **phonon** is used to describe a quantized lattice vibration. The optical phonon modes are classified into internal and external modes of vibration. Crystals are

constituted of a number of structural units. It may be considered that the force holding together the atoms within a group are much stronger than these keeping the various groups together[40]. The modes arising mainly from atomic oscillation within a group are termed **internal modes.** The molecular groups as a whole also perform rigid body motion. This vibration is called **external vibration** or **lattice vibration.** It is distinguished into two types, the first-ones are **translational modes** which involve the translation of molecular groups in the crystal. The second ones are **rotational** or **librational modes** which include the quasi-rotation of molecular groups about their centre of gravity. Therefore it needs the presence of polyatomic groups in the crystals. When a crystal is composed of a group of atoms forming an ion or molecule, its normal modes normally have the following modifications:

(a) Degenerate vibrational mode splitting,

(b) Increase in multiplicity due to the unit cell consisting of more than one molecule and

(c) Alternations in the selection rule[7].

It can be understood by considering the interaction of the environment of atoms where the vibrational potential energy

written as[40],

$$V = \sum_n V_n + \sum_n \sum_k V_{nk} + V_l + V_{ln} \qquad (1.11)$$

where terms represent as follows:

V_n is for internal coordinate, V_l for external coordinate, V_{nk} for two internal coordinates interaction and V_{nl} for interaction between external and internal coordinate.

1.11 CLASSIFICATION OF PHONON

Vibrations in a crystals are governed by **inter** and **intra** molecular interactions. The symmetry of a molecule in crystalline state is lower than the one in free state, because of intermolecular interaction. This lowering in symmetry may split degenerate vibrations and activate some vibrations in Infrared or Raman spectra which are otherwise inactive. Further, the spectra show bands due to translatory and rotatory motion of the molecule in the crystalline lattice. Generally, two group theoretical methods are used for the analysis of vibrational spectra and phonon classification. These are

(a) **Unit cell Approach**[43].

(b) **Site symmetry approximation**[44].

The application of these methods has been discussed by many authors[39,45,46]. Fately et al[47] proposed some practical rules for classification of phonons using site symmetry approach. A brief discussion of the two methods are given here. However, both the methods give the same results[48].

1.11.1 Unit Cell Approach

A crystal consisting of N primitive cells with n atoms per unit cell, has 3nN normal modes of vibration. These are distributed among 3n branches, out of which (3n-3) are **optical** and 3 **acoustic** branches. Mode frequencies depends upon the wave vector which can be chosen such that all its values lie within the first **Brillouin Zone** for each branch. However, other modes of vibration in which equivalent atoms more identically in phase are forbidden as fundamentals in Infrared and Raman scattering. This is due to the fact that the wave vector related with a photon is essentially zero with respect to the most of the phonons wave vector of the same energy except for ones near the Brillouin zone center. These constitute fundamental modes of vibration whose distribution, symmetry classification and optical activity can be enumerated only from the **unit cell** consideration in place of whole crystal.

All unit cells of lattice are in the same phase everywhere during period of execution of the fundamental optical modes.

So only 3n modes of unit cell are used for describing the dynamics of the entire crystal. Therefore, we consider the **factor group** which is made by the symmetry elements in the smallest unit cell (**Bravais cell**). It is always isomorphous with one of the 32 crystallographic point groups. The character table and the irreducible representations of the isomorphous point group corresponding to the space group of the crystal are needed in this procedure. m_k, the number of times of particular irreducible representation Γ_k is contained in another representation Γ, is given by

$$m_k = \frac{1}{m} \sum_j h_j \chi_k(R) \chi'_j(R) \tag{1.12}$$

where m is the order of the group, h_j is the number of group operations comprising the j-th class, $\chi_k(R)$ and $\chi'_j(R)$ are the characters of group operation R in the representations Γ_k and Γ respectively. The specific selection of the representation Γ and its suitable character $\chi'_j(R)$ are used for classification of normal modes. The selection rules are

$$\left.\begin{aligned} \frac{1}{m} \sum_j h_j \chi_k(R) \chi'_j(T) &= 0 \text{ IR forbidden} \\ &\neq 0 \text{ IR permitted} \end{aligned}\right\} \tag{1.13}$$

and

$$\left.\begin{aligned} \frac{1}{m} \sum_j h_j \chi_k(R) \chi'_j(\alpha) &= 0 \text{ Raman forbidden} \\ &\neq 0 \text{ Raman permitted} \end{aligned}\right\} \tag{1.14}$$

where T is used for dipole moment and α for polarizability tensor. The group character $\chi'_j(R)$ for different representations is given below[40].

All unit cell modes $\chi'_j(n_i) = w_R(\pm 1 + 2 \cos \phi_R)$ (1.15)

Acoustic modes (dipole moment) $\chi'_j(T) = \pm 1 + 2\cos \phi_R$ (1.16)

Translatory lattice modes $\chi'_j(T') = [w_R(s) - 1] (\pm 1+2 \cos \phi_R)$ (1.17)

Rotatory lattice modes $\chi'_j(R') = [w_R(s-p)]\chi'_j(P)$ (1.18)

Symmetric tensor $\chi'_j(\alpha) = (\pm 1 + 2 \cos \phi_R) 2 \cos \phi_R$ (1.19)

Here w_R is the number of atoms unchanged under the symmetry operation R, $w_R(s)$ is the number of structural group remains invariant under operation R, $w_R(s-p)$ is the number of polyatomic groups remains invariant under R, p is the number of monoatomic group, ϕ_R is the angle of rotation for R and positive and negative signs stand for proper and improper rotations respectively. For nonlinear polyatomic group we can write

$$\chi'_j(P) = 1 \pm 2 \cos \phi_R \tag{1.20}$$

and $\chi'_j(P) = \pm 2 \cos \phi_R$ for linear polyatomic groups. The number of internal modes can be found out by subtracting the

number of external modes (translatory + rotatory) from the total number of modes.

1.11.2 Site symmetry Approximation - correlation method:

According to Halford[44], the local potential is mainly responsible for the dynamics of mono and polyatomic groups in crystals. So he classified the normal modes by correlating the local symmetry point group, also called **site group** with the point group of free molecular ion. There, he neglected the interaction between the different groups in the same unit cell. The symmetry of the crystalline field around the site is described by site group. Thus the geometrical structure of a molecule or ion in a given site is defined by the symmetry of that site and it shows lower symmetry. Therefore, the site group is a subgroup of the unit cell or **factor group** which describes the symmetry of free molecules. For each equivalent set of atoms, a correlation chart can be set up between site groups and factor groups. Then site group species for the translations and rotations are correlated with species of the factor group. Lattice vibration species in the crystals are explicitly identified by this correlation which also allows the prediction of IR and Raman activity. The total reducible representation for lattice vibrations is obtained by summing up the reducible representations for each equivalent set of atoms or ions in the crystals.

For practical use of this method we consider the following useful terms[47]:

1. t^{γ} , R^{γ} = the numbers of translational and rotational coordinates in a site species γ. It can take value of zero, one, two or three, which are available from character table.

2. f^{γ} = degrees of vibrational freedom in every site of equivalent atoms, molecules or ions. It is calculated as

$$f^{\gamma} = n . t^{\gamma} \tag{1.21}$$

where n is the number of atoms, ions or molecules, in an equivalent site.

Similarly f_R^{γ} = degrees of rotational freedom which is found out by

$$f_R^{\gamma} = n . R^{\gamma} \tag{1.22}$$

3. a_{γ} = the degrees of freedom contributed by each site species γ to a factor group species ξ and found out as

$$f^{\gamma} = a_{\gamma} \sum_{\xi} {}^{\gamma}C_{\xi} \tag{1.23}$$

Similarly $$f^{\gamma} = a_{\gamma} \sum_{\xi} {}^{\gamma}C_{\xi} \tag{1.24}$$

4. $^{\gamma}C_{\xi}$ = the degeneracy of the species ξ of a factor group for site γ .

The reducible representation for internal vibrations of a molecular group can be obtained from the free state symmetry of that group. So free state symmetry group species are correlated with the site symmetry species and later the site symmetry species with the factor group species that yields reducible representation for internal vibrations, specifying the IR and Raman activity of the different internal vibrations. Finally, total representations for internal modes are added to the representation for lattice vibraions to get the reducible representation for total normal modes of vibrations of the crystals.

The irreducible representation of the crystals gives the number of lattice vibrations in each of the species of the factor group. The total irreducible representation of the crystals Γ is the combination of irreducible representation of each equivalent set of atom $\Gamma_{eq.set}$ where

$$\Gamma_{eq\ set} = \sum_{\xi} a_{\xi} \cdot \xi \tag{1.25}$$

we also write

$$\Gamma^{cryst}_{vib.} = \Gamma - \Gamma^{acout}. \tag{1.26}$$

Finally we get

$$\Gamma^{\text{mol. cryst.}}_{\text{vib.}} = \Gamma^{\text{cryst.}}_{\text{vib.}} + \Gamma_{\text{mol. vib.}} + \Gamma_{\text{lib.}} - \Gamma^{\text{acout.}} \qquad (1.27)$$

where $$\Gamma_{\text{lib.}} = \sum_{\xi} R_{a,\xi} \qquad (1.28)$$

1.12 INTERNAL MODES OF VIBRATION OF MOLECULAR GROUPS OF THE CRYSTAL UNDER STUDY

The atoms contained in the molecular group vibrate within nonrigid molecular motions. These are known as **internal vibrations.** For example, we discuss triammonium hydrogen disulphate (hereafter referred to as TAHS) crystal which is composed of NH_4^+, SO_4^{2-} ions. Those are XY_4 type molecular groups, showing tetrahedral (T_d) symmetry in the free state.

In the species of T_d point group, there are nine internal modes of vibration for a XY_4 type molecule and they are classified as

$$A_1 + E + 2F_2$$

In the first specy, the Y-atoms vibrate toward and away from the X-atom with A_1 symmetry, denoted as ν_1. Secondly, Y-atoms

move on the surface of a sphere with radius of X-Y bond distance, having E symmetry denoted as ν_2 and there are also two triply degenerate ν_3 and ν_4 having F_2 symmetry. ν_3 is the antisymmetric X-Y stretching mode where ν_4 is the asymmetric bending of X-Y bonds. All the four modes ν_1, ν_2, ν_3 and ν_4 are Raman active, ν_3 and ν_4 show IR activity as well. Fig. 1.3 shows four normal modes of vibration of tetrahedral molecules[49]. Using site symmetry approximation after Fateley et al[47], we found the distribution of normal modes among the factor group species which are summarized in the table 1.2.

1.13 ANHARMONICITY AND INTERACTION OF VIBRATIONS

The potential energy of any system can be expanded by Taylor series where the cubic or higher order terms cause the **anharmonic effect.** The **combinations** or **overtones** in the vibrational spectra which come from simultaneous changes of state by two or more quanta of vibrational energy, are the evidence of anharmonic effect. It can be explained in crystalline solids on the basis of **multiphonon processes**[50].

Molecular vibrations are affected by anharmonicity in two ways[49,50]. Firstly, the selection rule changes by $\Delta\nu = \pm 1, \pm 2$ ... and secondly, the space between the vibrational energy levels

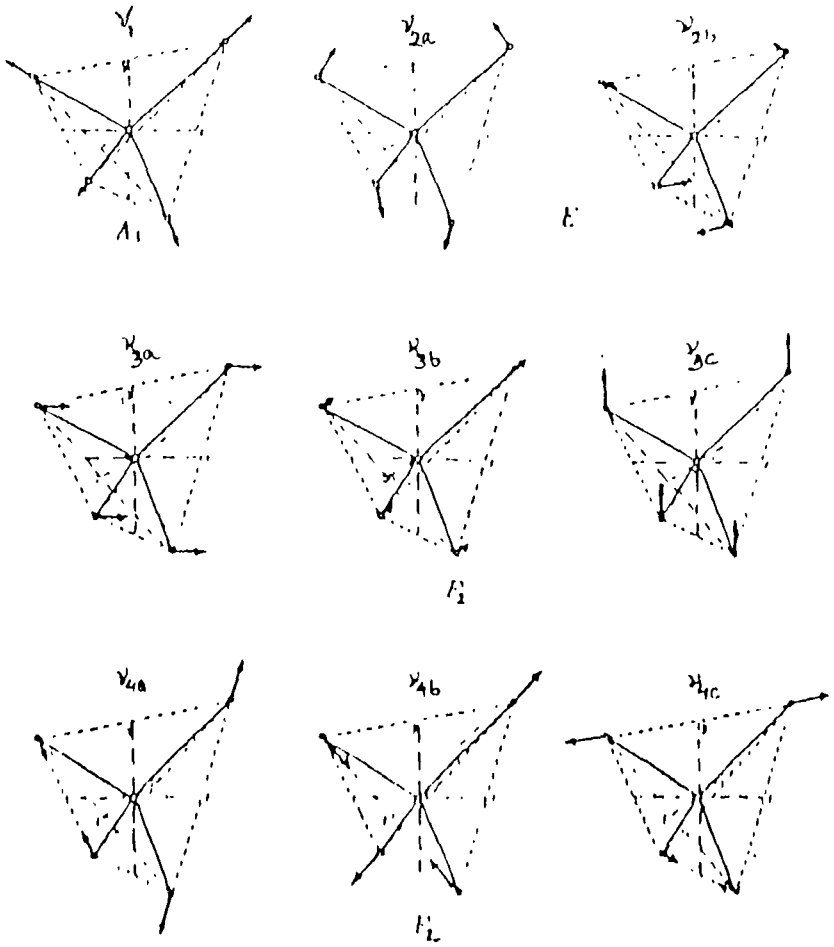

Fig. 1.3. Normal modes of vibration of a tetrahedral molecule.

Table 1.1 - Classification of Different Mode of a XY_4 Molecule under T_d symmetry

T_d	E	$8C_2$	$3C_2$	$6S_4$	6d	n	t	l	Internal modes		Activity	
									n_i	Designation	IR	Raman
A_1	1	1	1	1	1	1	0	0	1	ν_1	f	p(xx,yy,zz)
A_2	1	1	1	-1	-1	0	0	0	0	-	f	f
E	2	-1	2	0	0	1	0	0	1	ν_2	f	p(xx,yy,zz)
F_1	3	0	-1	1	-1	1	0	1	0	-	f (R_x,R_y,R_z)	f
F_2	3	0	-1	-1	1	3	1	0	2	ν_3, ν_4	p (T_x,T_y,T_z)	p(xy,yz,zx)

n - Total number of modes
t - Translatory modes
l - Libratory modes
n_i - Internal modes

is changed, so combination bands are also allowed. The overtone and combination band intensity are plainly related to the anharmonicity of vibrations. For anharmonicity, the splitting of degenerate level, **accidental degeneracy** and **Fermi Resonance** also occur.

There are two types of anharmonicity[51,52], **mechanical** and **electrical.** The first one comes for deviation from the harmonic form of potential energy for a given mode with potential energy written as

$$V = \frac{1}{2} K_2 Q^2 + K_3 Q^3 + K_4 Q^4 + \ldots\ldots\ldots \quad (1.29)$$

where Q is the normal coordinate and K_i is the force constant. Electrical anharmonicity is associated with the quadratic and higher terms contribution of the normal coordinate to the instantaneous dipole moment which can be written as

$$\vec{M} = M_0 + M_1 Q + M_2 Q^2 + \ldots\ldots\ldots \quad (1.30)$$

1.14 IR SPECTROSCOPY

1.14.1 General

IR Spectroscopy deals with the interaction of IR radiation

with matter. Actually its happens by the change of electric dipole moment (μ) of molecular unit for excitation to higher vibrational level[53]. It detects only long wave length polar excitation and supply fundamental information about SPT. For crystals it can be treated macroscopically because the wavelength λ for characteristic angular frequency of lattice excitations coupled with the IR radiation is much greater than the lattice constant a[35]. Cablentz[54] first made a systematic measurement of IR absorption in 1905.

An IR radiation propagated in the crystals must satisfy Maxwell's equations. Hence using Maxwell equation and Kramer-Kroning dispersion relations[55], one can find

$$\epsilon'(\omega) - 1 = \frac{4\pi e^2}{m} P \int_0^\infty \frac{n(\omega')\, d\omega'}{\omega'^2 - \omega^2} \tag{1.31}$$

$$\sigma(\omega) = \sigma(0) - \frac{\omega^2}{2\pi^2} P \int_0^\infty \frac{\epsilon'(\omega')\, d\omega'}{\omega'^2 - \omega^2} \tag{1.32}$$

where $\epsilon'(\omega)$ is real part of frequency dependent dielectric constant, $\sigma(\omega)$ is the frequency dependent conductivity, e and m is the charge and mass of the electron respectively and $n(\omega)$ is the number of harmonic oscillator. $\epsilon(\omega)$ gives the basic information about long wave length polar phonons which are determined by

reflection and transimission spectral measurements. Applying Maxwell's equation we can write for non conductive lossy medium

$$\epsilon' = n^2 - k^2 \text{ and } \epsilon'' = 2nk \geq 0 \tag{1.33}$$

where N = n-ik

where ϵ' and ϵ'' are real and imaginary parts of the dielectric constant and n, k are the real and imaginary parts of the refractive index of the medium. For normal incidence, the **amplitude reflection coefficient** is written as

$$r = \sqrt{R}\, e^{-i\theta} = \frac{1-n+ik}{1+n-ik} \tag{1.34}$$

and reflectivity coefficient R as

$$R = rr^* = \frac{(n-1)^2 + k^2}{(n+1)^2 + k^2} \tag{1.35}$$

Finally, extracting R and θ, we get

$$\epsilon(\omega) = \left(\frac{1+r}{1-r}\right)^2 \tag{1.36}$$

The basic information comes out from the theory of phonon or electron contribution to $\epsilon(\omega)$ [56]. In this theory the magnetic susceptibility (χ) is calculated from macroscopic electric field in a crystals, created by incident harmonic plane wave. Rigorous calculation of normal mode damping gives one longitudinal optic mode ($K \| E, \bar{\omega}_{Lj}$) and two transverse optic mode ($K \perp E, \bar{\omega}_{Tj}$). So we can write

$$\frac{\epsilon(\omega)}{\epsilon(\infty)} = \prod_{j=1}^{n} \frac{(\bar{\omega}_{Lj} - \omega)(\bar{\omega}^{*}_{Lj} + \omega)}{(\bar{\omega}_{Tj} - \omega)(\bar{\omega}^{*}_{Tj} + \omega)}$$

$$= \prod_{j=1}^{n} \frac{|\bar{\omega}_{Lj}|^2 - \omega^2 + i\omega\gamma_{Lj}}{|\bar{\omega}_{Tj}|^2 - \omega^2 + i\omega\gamma_{Tj}} \qquad (1.37)$$

where j runs over all normal modes from 1 to n and γ is the damping constant. From this equation we see that complex frequencies $\bar{\omega}_{Lj}$ and $\bar{\omega}_{Tj}$ are zeros and poles respectively on the dielectric spectrum. The Coulomb interaction between the ions depends on crystals surface condition which leads longitudinal-transverse mode splitting. Because of transverse nature of electromagnetic wave it cannot interact with longitudinal phonon in an infinite crystals. Hence longitudinal optical modes are inactive in IR absorption spectrum and observed in reflection spectrum. But transverse optical modes are optically active and can be observed in both absorption and reflection spectra.

The optical mode of a lattice is adequate to the motion of one type of atom, in phase relative to other, in long wavelength limit. Such motion in ionic crystals is related with strong electric moments. It can directly interact with the proper polarization electric field of incident radiation. Optical properties of this crystals are changed near the resonance frequency[40]. The crystal becomes totally reflecting in the neighbourhood of optical lattice mode region, that is known as **Reststrahlen effect.** It is clearly explained by IR dispersion relation

$$\epsilon(\nu) = \epsilon(\infty) + \frac{[\epsilon(0) - \epsilon(\infty)]\nu_0^2}{\nu_0^2 - \nu^2} \tag{1.38}$$

More accurate calculation is given by Huang[56]. The dispersion frequencies are same with the optical mode frequency ν_0 and the longitudinal frequency ν_l which is given by Lyddane-Sachs-Teller formula[53].

$$\nu_l = \left(\frac{\epsilon(0)}{\epsilon(\infty)}\right)^{1/2} \nu_0 = \frac{\epsilon(0)}{\epsilon(\infty)} \nu_t \tag{1.39}$$

For non ionic crystals, $\nu_l = \nu_t = \nu_0$. Ionic dielectric dispersion in the far IR region is treated only by quantum mechanics.

There are many experimental techniques in IR spectroscopy The technique mostly used in IR spectroscopy is transmission measurements on powder samples mixed with some transparent matrix and pressed into pellets. For the determination of IR dielectric function normally bulk reflectivity measurement is used. Power reflectivity R of the radiation can be measured directly by this method. For partially transparent single crystalline samples, transmission measurements are more useful and accurate because they are much more sensitive to changes of the optical constant[36].

1.14.2 Selection Rule

Selection rule for IR spectra is determined by the transition moment integral[53] which is quantum mechanically written as

$$[\mu]_{ij} = \int \Psi_i(Q_a)\, \mu\, \Psi_j(Q_a) dQ_a \qquad (1.40)$$

Here μ is the electric dipole moment in the electronic ground state, Ψ_i and Ψ_j are the vibrational eigen functions for the ground and excited states respectively and Q_a is the normal coordinate. If we resolve the dipole moment in X, Y and Z direction then one can write

$$
\begin{aligned}
[\mu_x]_{ij} &= \int \psi_i(Q_a)\, \mu_x\, \psi_j(Q_a)\, dQ_a \\
[\mu_y]_{ij} &= \int \psi_i(Q_a)\, \mu_y\, \psi_j(Q_a)\, dQ_a \\
[\mu_z]_{ij} &= \int \psi_i(Q_a)\, \mu_z\, \psi_j(Q_a)\, dQ_a
\end{aligned}
\qquad (1.41)
$$

when one of those integrals is not zero then the normal vibration associated with the normal co-ordinate Q_a is IR active. If all the integrals are zero then the vibrations are IR forbidden.

The ground state wave function ψ_i belongs to totally symmetric representation. So X, Y, Z and excited state must be of some representation to get the representation of their direct product totally symmetrical[57]. The simple IR selection rule is stated as **"A fundamental will be IR active if the normal mode which is excited belongs to the same representation as anyone or several cartesian coordiantes".** From character table we can say which cartesian coordinates are involved and IR activity of the fundamental will be found out. For asymmetric molecules all normal modes are IR permitted.

1.14.3 Analysis of IR spectra

Due to the directional properties of lattice, the nature of IR spectra varies with the orientation of the crystal with respect to the incident beam. Analysis of this dependence can be done by

group theoretical methods. From character tables, the IR reflectivity of different symmetry species for the point groups are known[39,57]. The optical constant can be related to the observed reflection spectrum near the dispersion frequency by Maxwell's equations. The soft mode and hard mode of the dielectric spectrum provide information about the phase transition mechanism.

1.15 RAMAN SCATTERING

1.15.1 General

Inelastic light scattering is very important to investigate the properties of matter. Light is scattered by a material due to fluctuation of the dielectric tensor of the material. Fluctuation of some of this quantity are enhanced near phase transitions[58]. So light scattering effect is an important tool for the study of phase transition. The static lattice structure can be determined with the help of symmetry information from polarized scattering[59].

In 1923, Smekal[60] studied the light scattering by a two quantized energy level system and give assertion about the side band existence in the scattered spectrum. Sir C.V. Raman and Krishnan[61,62] showed the side bands in scattered spectrum for liquid, like Benzene. They found the side bands in pairs

symmetrically shifted around the incident frequencies which are identical to some IR vibrational lines. In the same year, Landsberg and Mandelstam[63] observed same phenomena in quartz. The findings of Raman and Krishnan have been confirmed by Cabannes[64] and Recard[65]. This inelastic light scattering by molecular and crystal vibrations are known as **Raman scattering.** If ν is incident frequency then we got the scattered frequency, $\nu' = \nu \pm \nu_i$ where ν_i in the range of transition frequency between molecular rotational, vibrational and electronic level. The new wave numbers in the scattered spectrum are called **Raman lines** or **bands.** Raman bands at frequency $\nu_s = \nu - \nu_i$ below the incident frequency are termed **Stokes bands** and higher one i.e. $\nu_{AS} = \nu + \nu_i$, referred to as **Anti-Stokes bands.** A photon of frequency ν_i is absorbed and simultaneous emission of stokes photon of frequency $\nu_s = \nu - \nu_i$ is the stokes Raman scattering whereas Anti-Stokes photons of frequency $\nu_{AS} = \nu + \nu_i$, are emitted for de-excitation of the molecule from excited state to ground state. It depends on the numbers of molecule in the initial excited state. So Anti-Stokes radiation is weaker than Stokes emission.

A classical explanation of light scattering may be given in terms of the electromagnetic radiation by induced multipoles in the system for incident wave[66]. In most of the systems, only induced

electric dipole moment P is considered. It is related to the electric field E of the incident radiation as

$$\mathbf{P} = \boldsymbol{\alpha}.\mathbf{E} + \frac{1}{2}\boldsymbol{\beta}.\mathbf{EE} + \frac{1}{6}\boldsymbol{\gamma}.\mathbf{EEE} \tag{1.42}$$

where α is known as polarizability, β as hyper-polarizability and γ as second hyper-polarizability of the medium and all are tensor. The correct frequency dependence for Rayleigh and Raman scattering can be found from first term of equation (1.42). In matrix notation we can write as

$$[P] = [\alpha]\,[E] \tag{1.43}$$

The polarizability is a function of the nuclear coordinate. So polarizability can be expressed in a Taylor series in terms of normal coordinates of vibration which is written as,

$$\alpha_{ij} = (\alpha_{ij})_0 + \sum_k \left(\frac{\delta\alpha_{ij}}{\delta Q_K}\right)_0 Q_k + \frac{1}{2}\sum_{K,L}\left(\frac{\delta^2\alpha_{ij}}{\delta Q_k \delta Q_l}\right)_0 Q_k Q_l \tag{1.44}$$

where $\dfrac{\delta\alpha_{ij}}{\delta Q_K}$ is called derived polarizability tensor.

In harmonic approximation for space fixed molecule, we can write

$$P_{xo}(\omega_o \pm \omega_k) = [(\alpha'_{xx})_k E_{xo} + (\alpha'_{xy})_k E_{yo} + (\alpha'_{xz})_k E_{zo}] Q_{ko}$$

$$P_{yo}(\omega_o \pm \omega_k) = [(\alpha'_{yx})_k E_{xo} + (\alpha'_{yy})_k E_{yo} + (\alpha'_{yz})_k] Q_{ko} \qquad (1.45)$$

$$P_{zo}(\omega_o \pm \omega_k) = [(\alpha'_{zx}) E_{xo} + (\alpha'_{zy})_k E_{xo} + (\alpha'_{zz})_k] Q_{ko}$$

where Q_{ko} is normal coordinate amplitude ω_o is the incident frequency and ω_k is the molecular frequency. The light scattering process has directional and polarization properties. Porto[67] has proposed a notation for describing polarization data from single crystals. Details of the quantum mechanical treatment of Raman scattering has been outlined by Long[66] and Brandmüller and Moser[68].

We are interested to investigate the phase transition of solids. So we consider the light scattering in the vicinity of phase transition. Due to temporal and spatial fluctuation of the dielectric tensor in the medium, the scattered light frequency ω_s and wave vector $\mathbf{k}_s$ are not same as the incident light frequency ω_I and wave vector $\mathbf{k}_I$. In the neighbourhood of phase transition, fluctuation of some physical quantity called order parameter which plays the main role in light scattering intensity[58]. Taking temporal and spatial dependence, we get the spectral power density as

$$I_{ij}(q,\Omega) \propto [n(\Omega) + 1] \, \mathrm{Im}\chi^{\epsilon}_{ij}(q,\Omega) \tag{1.46}$$

where $\chi^{\epsilon}_{ij}(q,\Omega)$ is the generalized susceptibility, $n(\Omega)$ is the B.E. occupation number at frequency Ω and $\Omega = \omega_I - \omega_S$ $q = k_I - k_S$.

The fluctuation of dielectric tensor can be expressed as

$$\epsilon_{ij}(r,t) = \epsilon_{ij}(o) + \delta\epsilon_{ij}(r,t) \tag{1.47}$$

where $\delta\epsilon_{ij}(r,t)$ is the deviation from equilibrium value $\epsilon_{ij}(o)$. In terms of order parameter (η) we can write

$$\delta\epsilon_{ij} = e_{ij}\eta \tag{1.48}$$

where e_{ij} is polarization direction.

Therefore, for single soft mode of vibration we get

$$I_{ij}(q,\Omega) \propto [n(\Omega) + 1] \, |e_{ij}\eta|^2 \, \frac{\Omega\Gamma}{(\Omega_o^2 - \Omega^2) + \Omega^2\Gamma^2} \tag{1.49}$$

where Γ is the damping constant.

In many cases, this single soft mode theory does not yield satisfactory results. Yacoby et al[69] have given some explanation for the discrepancy between theory and experiment.

The peak intensities and line-width of the bands have been measured by least square fitting of the experimentally observed multiple band structure. Here we have assumed that it was composed of multi-Lorentzion bands such that the overall contour is given by

$$I = \sum_n I(\nu_{oi})\, b_i^2 /[b_i^2 + (\nu - \nu_{oi})^2] \qquad (1.50)$$

where ν_{oi} is the peak frequency and b_i is the half-width at half maximum height (HWHM) of the i-th band. The full width at half maximum (FWHM) so obtained was corrected for the finite instrumental slit width using the formula[70].

$$(\delta_i)_t = (\delta_i)_a \; [1-[/s/(\delta_i)_a]^2] \qquad (1.51)$$

where $(\delta_i)_t$ is the corrected FWHM of the i-th band, $(\delta_i)_a$ is the apparent FWHM of the i-th band and S is the instrumental slit width in cm^{-1}.

1.15.2 Selection Rule for Raman Scattering

According to quantum mechanics, the vibrations are Raman active only when one of the components of polarizability tensor (α) changes during vibration. It can be determined by transition moment integral defined as

$$[\alpha]_{fi} = \int \psi_f(Q_a) \alpha \psi_i(Q_a)\, dQ_a \qquad (1.52)$$

where ψ_f and ψ_i are wave functions of final and initial molecular states and Q_a is the normal coordinate. The polarizability tensor has six components, so equation (1.52) resolved into six integrals as follows.

$$\begin{aligned} [\alpha_{xx}]_{fi} &= \int \psi_f(Q_a) \alpha_{xx} \psi_i(Q_a)\, dQ_a \\ [\alpha_{yy}]_{fi} &= \int \psi_f(Q_a) \alpha_{yy} \psi_i(Q_a)\, dQ_a \\ [\alpha_{yz}]_{fi} &= \int \psi_f(Q_a) \alpha_{yz} \psi_i(Q_a)\, dQ_a \end{aligned} \qquad (1.53)$$

If all the integrals are zero then the vibration is Raman inactive. In the integral, α is one of the quadratic functions of the cartesian coordinates like X^2, Y^2, Z^2, XY, YZ, ZX, X^2-Y^2 etc.

If the normal mode belongs to the same representation as one or more polarizability tensor components then the fundamental

transition will be Raman active. Actually, all modes from totally symmetric classes are always Raman active. If there is a centre of inversion element in the group then all antisymmetric normal modes are Raman inactive. All Raman active modes combine with each one of the modes which come under the totally symmetric class to give Raman active combination tones.

1.15.3 Analysis of Raman Spectra

The nature of Raman spectra depends on the orientation of the crystals with respect to the radiation beams. These effects can be analysed by group theoretical methods. From character tables we can get Raman activity of vibrations of different species of a point group. Loudon[71] gives Raman tensors for the Raman active species of all 32 crystallographic point groups with respect to three mutually perpendicular axes, defined by Nye[72]. The optical properties of crystals can be understood in terms of principal axes of indicatrix[69,73].

REFERENCES

1. Bruce A.D. and Cowlay R.A. "Structural Phase Transitions" Taylor and Francis Ltd., London (1981).
2. Krishnan R.S., Phys. News **9** 56 (1978).
3. Scott J.F., Rev. Mod. Phys. **45** 83 (1974).
4. Steigmier E.F., Ferroelectrics **7** 65 (1974).
5. Nakamura T., Ferroelectrics **9** 159 (1975).
6. Fleury P.A. In "Proceeding of the Third International Conference on Light Scattering in Solids" ed. by M.Balkanski, R.C.C. Leite and S.P.S. Porto; Flammarion, Paris (1976).
7. Hossain A. "M.Phil Dissertation", A.M.U., Aligarh, India (1990).
8. Rao C.N.R. and Rao K.J. "Phase Transition in Solids" McGraw-Hill, INC., New York (1978).
9. Landau L. and Lifshitz E.M. "Statistical Physics" Pergamon, Oxford (1959).
10. Tisza L. In "Phase Transformations in Solids" ed. by Smoluchowski R., Mayer J.E. and Weyl W.A., John Wiley & Sons INC., New York, Chapman and Hall Ltd., London (1951).
11. Ehrenfest P., Leiden Comm. Suppl. **75b** (1933).
12. Müller K.A. In "Structural Phase Transition; Vol. - I" ed. by K.A. Müller and H. Thomas, Springer-verlag, Berlin (1981).
13. Thomas H., IEEE Trans. Magn. **5** 874 (1969).
14. Bürger M.J. In "Phase Transition in Solids" Willey, New York (1951).
15. Iqbal Z. In "Vibrational Spectroscopy of Phase Transition" ed. by Zafer Iqbal and F.J. Owens, Academic Press INC. (1984).

16. Rowe J.M., Rush J.J., Chesser N.J., Michel K.H. and Naudts J., Phys. Rev. Lett. **40** 455 (1978).
17. Michel K.H. and Naudts J., Phys. Rev. Lett. **39** 212 (1977).
18. Michel K.H. and Naudts J., J. Chem. Phys. **67** 547 (1977).
19. Elliott R.J., Harley R.T., Hayes W. and Smith S.R.P., Proc. R. Soc. London **A328** 217 (1972).
20. Pytte E., Ferroelectrics **7** 193 (1974).
21. Peierls R.E. "Quantum Theory of Solids" Oxford Univ. Press (Clarendon) London and New York. (1955).
22. Pytte E., Solid State Commun. **8** 2101 (1970).
23. Dorner B., Axe J.D. and Shirane G., Phys. Rev. B **5** 1950 (1972).
24. Riste T. "Electron Phonon Interactions and Phase Transitions" Plenum, New York (1978).
25. Fleury P.A. and Lyons K. In "Structural Phase Transition, Vol.-1" ed. by K.A. Müller and H. Thomas, Springer-verlag, Berlin (1981).
26. Mcmillan W.L., Phys. Rev. B **12** 1187 (1975).
27. Crussard C. "International Conference on the Physics of Metals" Amsterdam (1948).
28. Hayes W. and Loudon R. "Scattering of Light by Crystals" John Wiley & Sons, New York, (1978).
29. Raman C.V. and Nedungadi T.M.K., Nature **145** 147 (1940).
30. Cochran W., Adv. Phys. **9** 387 (1960).
31. Anderson P.W., Fiz Dielectr. Acad. Nauk. SSSR 290 (1960).
32. Cowley R.A., Adv. Phys. **12** 421 (1963).
33. Cowley R.A. In "Proceedings of the International Conference on Lattice Dynamics" ed. by M. Balkanski Flammarion, Paris (1977).
34. Fröhlich H. "Theory of Dielectric" Oxford Univ. Press (Clarendon), London and New York (1949).

35. Petzelt J. and Dvořák V. In "Vibrational Spectroscopy of Phase Transition" ed. by Zafer Iqbal and F.J. Owens, Academic Press INC. (1984).

36. Petzelt J. and Dvořák V., J. Phys. C. **9** 1571 (1976).

37. Petzelt J. and Dvořák V., J. Phys. C. **9** 1587 (1976).

38. Gervais F. and Pirion B., Phys. Rev. B. **11** 3944 (1975).

39. Turell G. "Infrared and Raman Spectra of Crystals" Academic Press, London (1972).

40. Mittra S.S. In "Optical Properties of Solids" ed. by Sol. Nudelman and S.S. Mittra; Plenum Press, New York (1969).

41. Kittel C. "Introduction to Solid State Physics". John Wiley & Sons INC., New York (1966).

42. Wilson E.B., Decius Jr. D.C. and Cross P.C. "Molecular Vibration" McGraw-Hill, New York (1955).

43. Bhagavantam S. and Venkatarayudu T., Proc. Ind. Acad. Sci. **A9** 224 (1939).

44. Halford R.S., J. Chem., Phys. **14** 8 (1948).

45. Bhagavantam S. and Venkatarayudu T. "Scattering of Light and the Raman Effect", Chemical Publication Co., New York.

46. Mittra S.S., Solid State Phys. **13** 1 (1962).

47. Fately G.W., Dollish R.F., McDevitt T.N. and Bentley F.F. "Infrared and Raman Selections Rules for Molecular and Lattice Vibrations: The Correlation Method" Wiley-Interscience, A division of John Wiley & Sons INC., New York, (1972).

48. Winston H. and Halford R.S., J. Chem. Phys. **17** 607 (1949).

49. Hertzberg G. "Molecular Spectra and Molecular Structure: Vol. - II" D. Van Nostrand Co., INC. Princeton, New Jersey, (1945).

50. Mittra S.S., J. Chem. Phys. **39** 3031 (1963).

51. Foldes A. and Sandorfy C., J. Mol. Spectrosc. **20** 262 (1966).

52. Herman R.C. and Shuler K.E., J. Chem. Phys. **22** 262 (1966).

53. Nakamato K. "Infrared and Raman Spectra of Inorganic and Coordination Compounds" John Wiley, New York (1978).

54. Coblentz W.W. "Investigation of Infrared Spectra" carnegie Institute Publications, Washington D.C. (1905).

55. Landau L.D. and Lifshitz E.M. "Electrodynamics of Continuous Media" Pergamon, Oxford (1960).

56. Born M. and Huang K. "Dynamical Theory of Crystals Lattices" Oxford Univ. Press, London and New York (1954).

57. Cotton F.A. "Chemical Applications of Group Theory" John Wiley & Sons. INC., New York (1976).

58. Wang C.H. In "Vibrational Spectroscopy of Phase Transitions in Solids" ed. by Zafar Iqbal and F.J. Owens, Academic Press INC. (1984).

59. Worlock J.M. In "Structural Phase Transitions and Soft Modes" ed. by E.J. Samuelsen, E. Andersen and J. Feder, Universitetsforlaget, Oslo-Borgen-Tromsö (1971).

60. Smekal A., Naturmiss **11** 873 (1923).

61. Raman C.V. Ind. J. Phys. **2** 387 (1928).

62. Raman C.V. and Krishna K.S., Nature **121** 501 (1928).

63. Landsberg G. and Mandelstam L. Naturmiss **16** 557 (1928).

64. Cabannes J., Compt. rend **186** 1201 (1928).

65. Recard Y., Compt. rend **186** 1107 (1928).

66. Long D.A. "Raman Spectroscopy" McGraw-Hill International, London (1977).

67. Damen T.C., Porto S.P.S. and Tell B., Phys. Rev. **142** 570 (1960) and Phys. Rev. **144** 771 (1966).

68. Brandmüller J. and Moser H. "Einführung in die Raman Spektroskopic" Steinkopf Verlag, Darmstadt, (1962).

69. Yacoby Y., Cowley R.A., Hosea T.J., Lockwood D.J. and Taylor W., J. Phys. C: Solid State Phys. **11** 5065 (1978).

70. Tanabe K., Spectrochim. Acta. Part **A40** 437 (1984).

71. Loudon R., Advn. Phys. **13** 423 (1964).

72. Nye J.F. "Physical Properties of Crystals" Clarendon Press, Oxford (1957).

73. Wahlstrom E.E., "Optical Crystallography" John Wiley, New York (1969).

CHAPTER - II

EXPERIMENTAL TECHNIQUE

EXPERIMENTAL TECHNIQUE

2.1 INTRODUCTION

This chapter describes in brief the crystal preparation technique under study, the description of equipment used for Raman and IR measurements. Raman spectra have been measured at room temperature and below down to 125 K. The IR spectra of powder sample have been taken at room temperature.

2.2 PREPARATION AND GROWTH OF CRYSTALS

Triammonium hydrogen disulphate (hereafter referred to as TAHS) single crystals were prepared by slow evaporation of aqueous solution, containing 40.8 wt% of $(NH_4)_2\ SO_4$ and 24.0 wt% of H_2SO_4 at about 30° C[1]. Crystals were purified by recrystallization process and obtained in the form of optically transparent hexagonal plates of 15 x 10 mm^2 and about 3 mm thickness.

2.3 EXPERIMENTAL SET UP FOR RAMAN SPECTRA MEASUREMENT

The experimental set up consisted of a source, 165 Ar^+ laser from Spectra physics, a 1403 Spex double monochromator, a photomultiplier detector and Spex datamate. The block diagram is

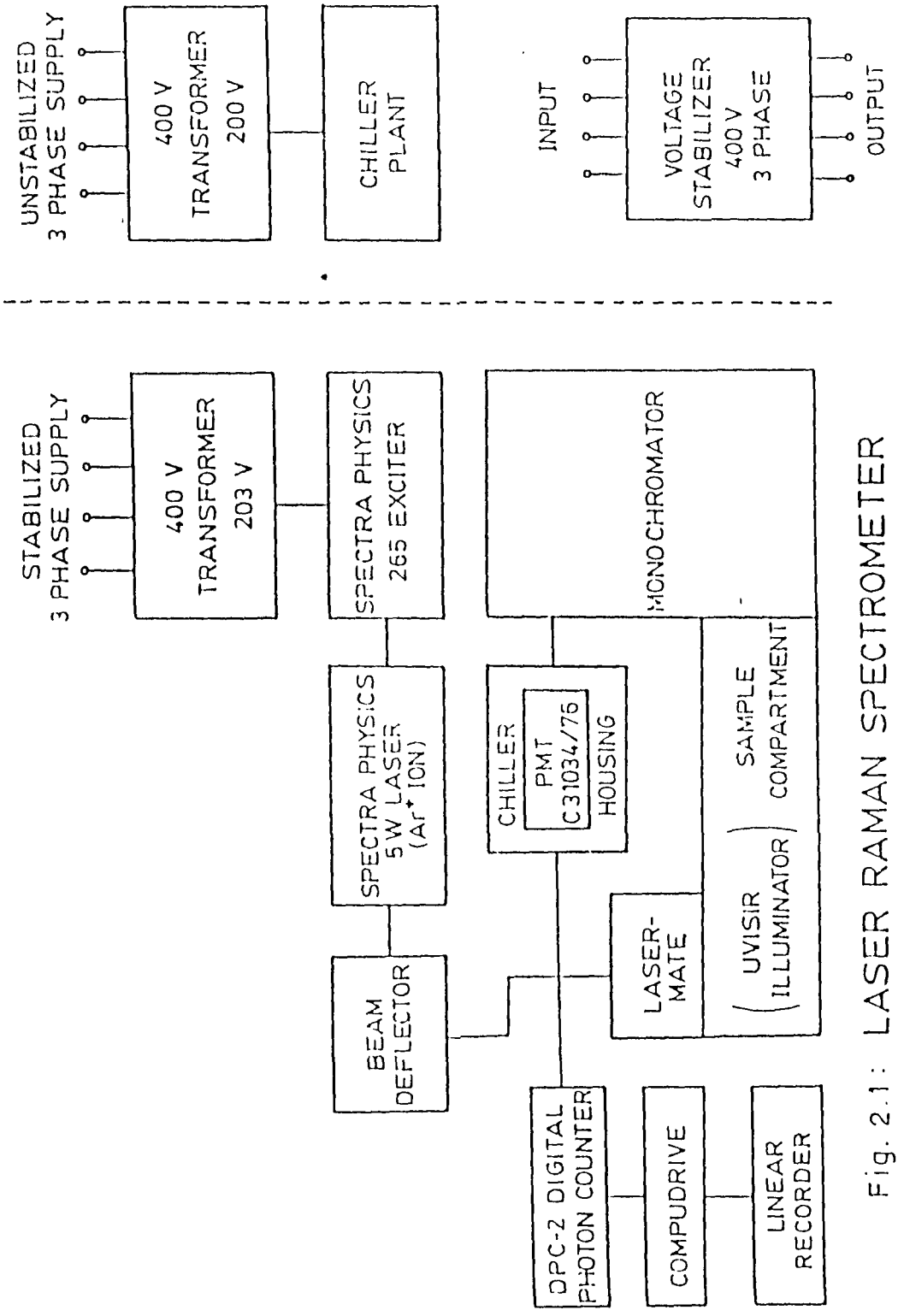

Fig. 2.1 : LASER RAMAN SPECTROMETER
(BLOCK DIAGRAM)

shown in Fig. 2.1. In the following paragraph, a brief description of main components of the experimental set up, measurements of polarized Raman spectra at different temperature, Experimental difficulties and its preventative measures have been described.

2.3.1 Source

The 4880 Å radiation with constant power of 100 mW from 5 watt spectra physics **Model 165-Ar^+** laser was used to excite the crystal. Technical and operational details are given in manual[2]. The three phase mains voltage was stabilized first to 400 volts from the main line to get stabilized three phase 203 volts for the laser power supply. This was achieved by three single phase 8.3 KVA (each) voltage stabilizers which are converted to 203 volts by a power transformer. The laser head and its power supply were cooled by circulating distilled water in a closed loop and maintained at a temperature at 20°C by the HX-500 chilling plant. The heat of the chilling plant is dissipated by tap water.

2.3.2 Spex Ramalog System

The main part of the spectrometer are a **lasermate, UVISIR illuminator** and a **double monochromator**[3]. The optical diagram of the set up for Raman measurements is shown in Fig. 2.2.

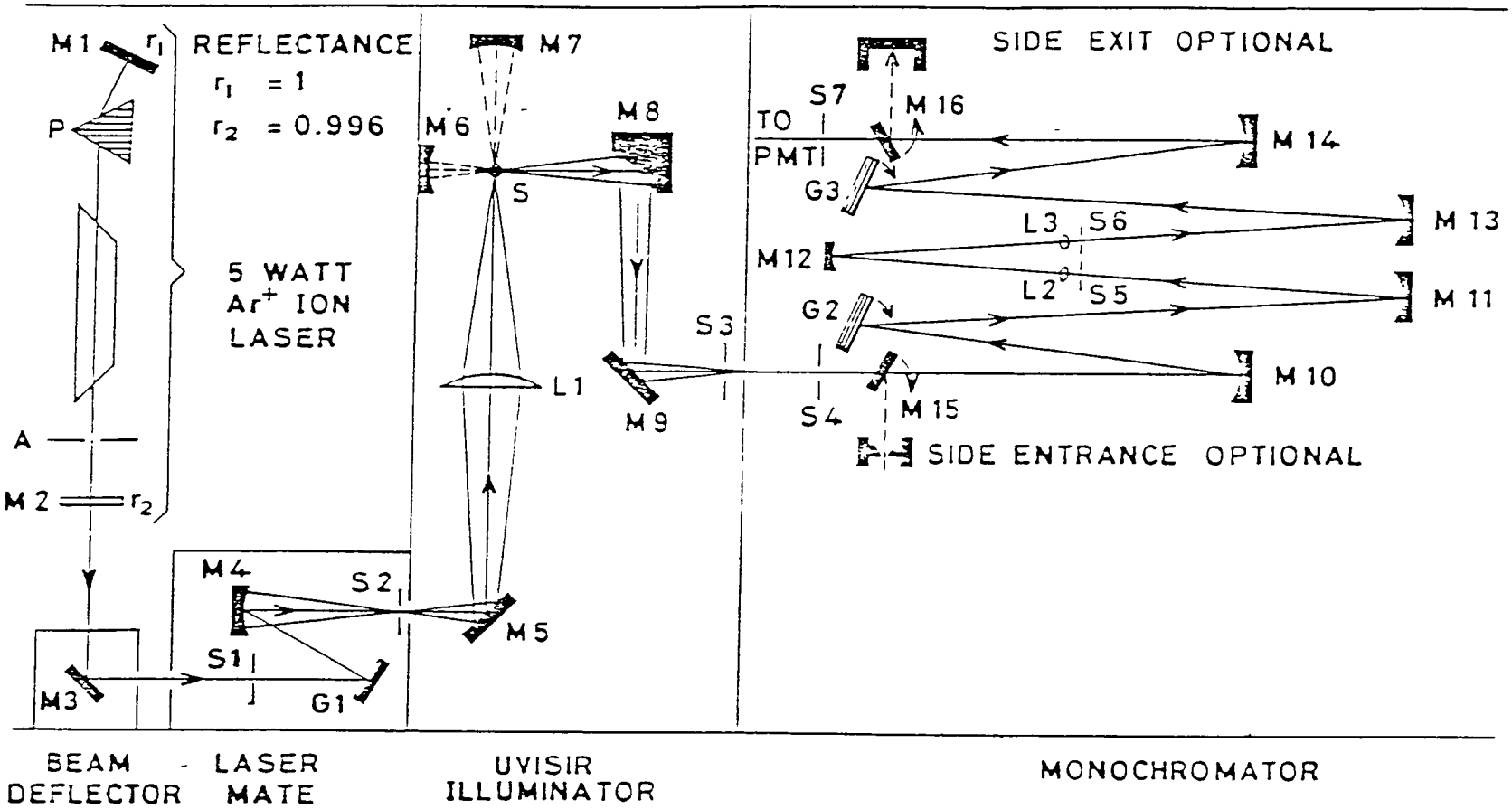

P: Prism; A: Aperture; M1-M3, M5, M9, M15, M16: Plane Mirrors; M4, M6, M7, M10-M14: Concave Mirrors; M8: Elliptical Collector Mirror; S1-S7: Slits; G1-G3: Gratings; L1: Fused Silica Condenser Lens; S: Sample; L2, L3: Optical Filter; PMT: Photomultiplier Tube.

Fig. 2.2. Optical Diagram of Spectra Physics Laser and Ramalog 1403 Spectrometer.

To record the Raman Spectra the excitation laser beam of 4880 Å is passed through the lasermate which filters out the plasma lines. After filtration it enters the UVISIR illuminator, where a small focal length fused-silica condensing lens is used to focus the beam of 1.5 nm diameter to a spot of $\sim$ 10 μm diameter on the sample. A polarizer is used with laser source to allow the particular polarized laser beam. An elliptical mirror is used to collect the scattered beam and focussed on to the entrance slit of the monochromator. An analyzer is placed in the path of scattered light to analyze the polarization of the scattered beam. A quartz wedge-depolarizer is placed after the analyzer to eliminate the polarization dependent efficiency of the grating.

The scattered radiation entering the slit is analyzed spectrally by double monochromator. The Spex-1403 double monochromator is of Czerny-Turner type with scanning range from 31000 cm^{-1} to 11000 cm^{-1}. An accuracy of $\pm$ 1 cm^{-1} in 10000 cm^{-1}, resolution of 0.15 cm^{-1} and spectral repeatability can be done successfully by this instrument. The double monochromator has a relative aperture of f/7.8 with two holographic gratings ruled with 1800 lines/mm and blazed at 5000 Å, where f is the focal length of the lens. An RCA-31034-02 photomultiplier tube (PMT) was used to get the spectral data. For reducing the dark current

caused by thermionic emission from the photo cathode, PMT has been cooled to 20°C by the thermoelectric cooling device. The PMT consists of gallim arsenide chip as its photocathode, an ultraviolet transmitting glass window and an inlines copper-beryllium-dynode structure consisting of eleven dynodes.

An 8 bits microcomputer **'Spex-Datamate'** was used for data processing and controlling the spectrometer. The spectral data were manipulated for the desired frequency range by in-built software. There are also arrangements to store the input and output data in the 4K data point storage in any of its eight variable length files. The stored data are plotted in a **strip chart recorder.** It is also possible to record the spectra directly on the strip chart recorder. Datamate also supplies high voltage to PMT (-1750 volts) with a stability of $\pm$ 0.002% after half an hour of warm up.

2.3.3 Scan of Raman Spectra

For polarized Raman spectra of single crystals, the samples have been cut in rectangular plates shape so that the faces of the plate are normal to the crystal axes. The indicatrix axes were indentified by polarizing microscope. The rectangular plate of

crystals are mounted on a sample holder in a way that two axes lie along the direction of incident and scattered radiation. The third axis is along in the direction of electric vector of incident beam. The measurement of various components of the polarizability tensor can be performed by recording spectra for different orientations of crystal axes relative to the direction of incident and scattered light and direction of electric vector in the incident and scattered beam. For complete study of Raman tensors, a minimum number of geometries is needed which depends on the crystal symmetry[4].

Porto[5] has given a notation to define the geometry used in Raman measurements. Using four symbols one can define the above geometry that are the propagation direction of the incident radiation, the direction of electric vector of the incident beam, the direction of electric vector of the scattered beam and the direction of propagation of scattered radiation. For example in the notation X(YZ)Y, X and Y outside the parenthesis denote the direction of propagation of incident and scattered light respectively, whereas the symbol Y and Z inside the parentheses indicates the direction of electric vector in the incident and scattered light respectively. The scattering tensor component is defined by the two symbols inside the parentheses.

2.3.4 Measurement of Raman Spectra at Different Temperature

For below room temperature measurement of Raman spectra of TAHS, an air products closed-cycle Helium cryocooler **Displex Model CSA-202E** was used. In that instrument we can cool the sample from 300 K down to 10 K. It consists a compressor model 202 and DE 202 Expander module, which are shown in Fig. 2.3. The temperature of the sample is controlled by a digital temperature controller model **APD-E**, with the accuracy of $\pm$ 3K. The temperature sensing and monitoring is precalibrated by gold chromel thermocouple. The refrigeration of the cryocooler is 1.8 Watts at 20 K. Conductive glue was used on the sample holder to mount the crystals. For thermal insulation, the system was evacuated upto 10^{-5} torr. by a **Hind-Hivac** diffusion pump. A home made heavy stainless steel stand was used to support the expander · module. The shaft of the stand was arranged in such a way that it can be moved back and forth in two perpendicular directions in horizontal plane. Up or down movements could also be possible through a gear and screw arrangement in the arm of the stand.

2.3.5 Factor affecting the Intensity of the recorded Spectrum

There were a considerable, unrelated factors that affect the

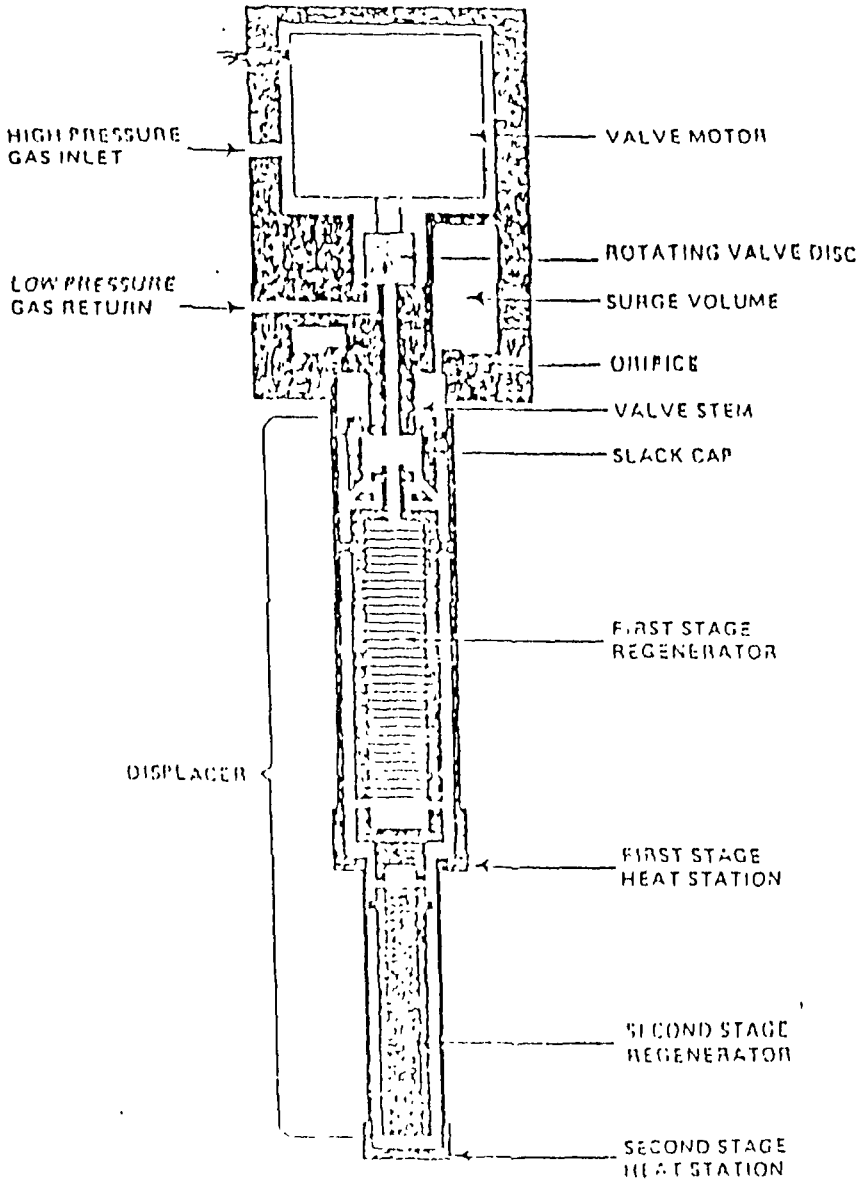

Fig. 2.3. A simplified diagram of the Air Products model DE 202 Expander module of the closed-cycle Helium Cryocooler.

type and quality of the spectra discussed below:-

1. **Raman Scattering:**

From theory we know that the Raman scattering from a particular set of molecules is directly proportional to the intensity of the incident light to the fourth power of the exciting laser line frequency and to other parameters, mainly molecular, over which experimentalist has little control. So high power lasers are used for weak spectra but there are some limitations.

2. **Diffraction grating efficiency:**

The efficiency of the grating in a particular order is at a maximum at the blaze wave length and falls on either side of that wave length. The blaze wave length depends on laser source.

3. **Photomultiplier Tubes**

The Raman light emerging from the exit slit of the spectrometer is generally detected by a photomultiplier tube having an S-20 type spectral response. The efficiency of the photomultiplier tube falls very rapidly at long wave length.

4. **Spectral Slit Width:**

At the time of scanning of the spectrum, the slit width remains constant. But the actual slit width continuously varies through out the scanning. The slit setting dial reads the slit width at 6328 Å . A correction table was supplied with the instrument.

5. **Discrimination:**

The discrimination of the spectrometer is a measure of the stray light in the monochromator.

6. **Sample Illuminating Methods:**

2.3.6 Calibration of the Spectrometer:

The spectrometer can be calibrated by using the emission spectrum of Neon. The best available values of wavelengths of the Neon emission lines are given by Loader[6]. The Neon emission spectrum is not convenient standard for routine use in Raman Spectra. IUPAC commission on molecular structure and spectroscopy recommended indene and polystyrene for routine calibration . The positions of the indene Raman emissions were located accurately and enabling vibrations which were active in both IR and Raman to be

identified. The correct frequencies at these vibrations are listed in the IUPAC tables.

2.3.7 Precautions:

1. Eye damage can be result from accidental reflection of the laser beam from polished surface, so safety goggles should be used.

2. Low temperature cell window and lens should be clean and free from grease and finger prints. Otherwise it increases the fluorescent background of the spectrum.

3. An e.h.t. voltage be applied to the PMT to destroy the room light effect completely. For scanning near exciting line, it also to be noted that the tube is not exposed to an excessively high intensity of light.

2.4 IR INSTRUMENT:

The optical mull principle for IR spectrometers was introduced in 1942 and other successful systems also were developed[7]. All the instruments have a common double path of source illuminating the monochromator entrance slit with a rotating mirror by means of flickering alternatively between the reference

and sample path. The detector responds only for unequal intensity of the two beams. For any unbalance, the light attenuator move in or out of the reference beam to restore balance and the recording systems respond. The recording pen is attached with the light attenuator, so it records the sample percent transmission. In the FIR region, the IR transmission spectra at room temperature were recorded by a commercial Perkin-Elmer 580 spectrometer with a dry air purging system. Many authors have discussed details of this instruments[8]. For calibration of the frequency scale we used the spectrum of polystyrene. The optical diagram of the used system is shown in Fig. 2.4[9].

2.4.1 Measurement of IR Spectra:

Powdered (micro crystalline) samples on KBr pellet and Nujol mull were used to record the NIR transmission spectra at room temperature. Extremely thin ($\sim .1\ \mu$) samples are needed for fine transmission spectra because fundamental lattice modes have high absorption power. However, the single crystal IR study can be done by specular reflectance or by attenuated total reflection techniques[8,10,11]. Normally, the Nujol mull[9,13] and Pressed disc[14] techniques are used for recording the transmission spectra in powder form. The particle size of the sample should be less than

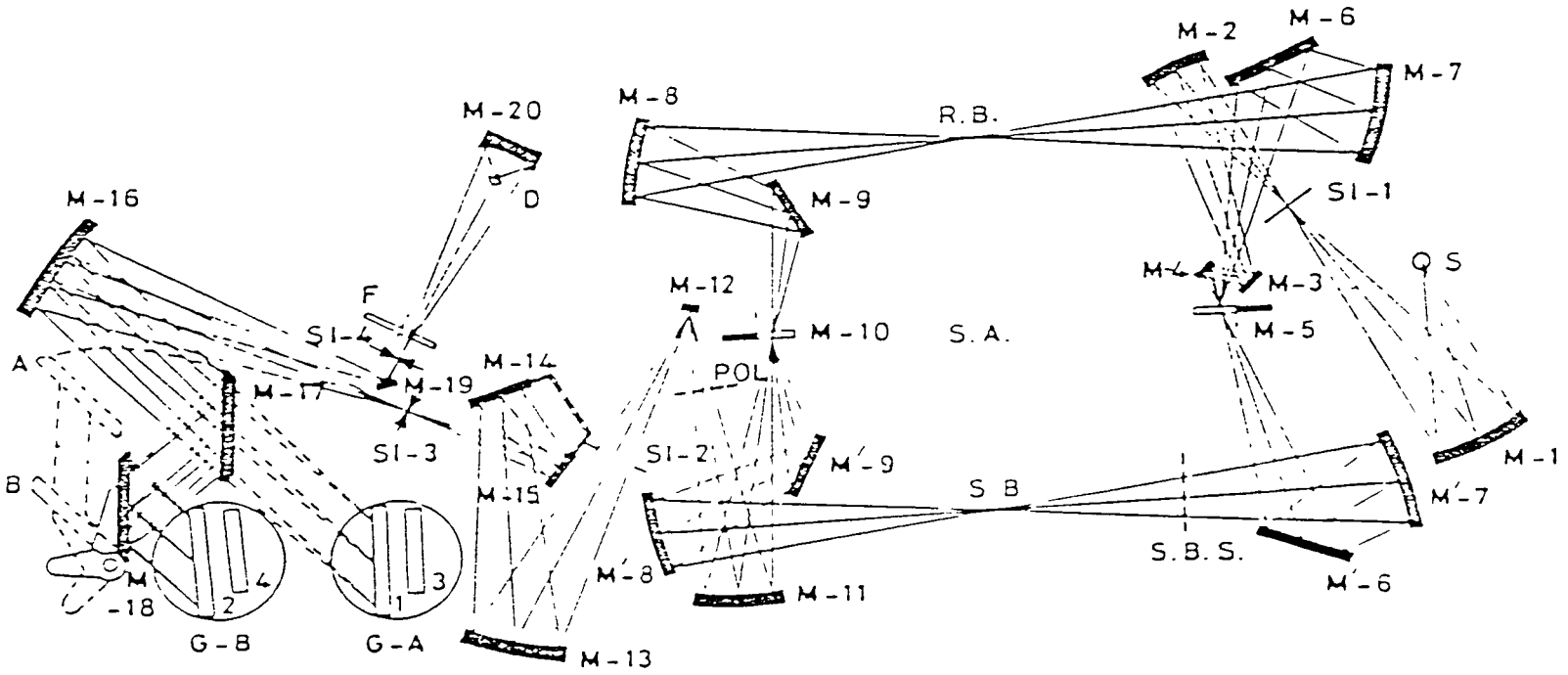

S:Source; M1,M2,M4,M7,M'7,M8,M'8,M11-M13:Toroid Mirrors; M5,M10:Chopper Mirrors; M3,M6,M'6,M9, M'9,M14,M15,M17,M19:Reflection and Scatter Grating Surface Mirrors; M16:Paraboloid Mirror; M20: Elipsoid Mirror; G-A,G-B.Grating Tables; SI-1:Baffle and Seconcary Source, SI-2:Pupil Baffle; SI-3: Entrance Slit; SI-4:Exit Slit, POL:Polarizer Accessory; F:Optical Filter; D:Detector; SBS:Sample Beam Shutter; SB:Sample Beam; SA:Sample Area; RB:Reference Beam.

Fig. 2.4. Optical Diagram of Perkin-Elmer Model 580 Infrared Spectrophotometer.

the incident radiation wavelength otherwise it shows some serious effects in the spectra. It also minimizes the scattering as well as **Christionsen effect** which are generally present in the spectra.

2.4.2 The Nujol-Mull Technique:

This technique has been performed by grinding the sample in mineral oil like - Nujol, to make thin paste. It behaved as a coating around the sample and match easily the refractive indices of the solid than air. For uniform cream like suspension, a thin layer is packed tightly between the well polished NaCl, KBr pellets and mounted in the sampling area of the spectro-photometer. To compensate the absorption bands of Nujol, we placed a few drop of Nujol in another demountable cell between the pellets. Nujol, cannot give fruitful information around 2915, 1462, 1376 and 719 cm^{-1} frequency because of its absorb bands at that frequencies.[15] There were used another mulling agents, such as Fluerolube or hexachlorobutadiene (HCBD).

The sufficient control over sample thickness, dispersion uniformity and paste density were not maintained in the mull technique. Even with the use of international standards, the mull technique will not give the fruitful quantitative analysis. However, it is used for qualitative analysis of the samples.

2.4.3 The Pressed disc (Pellet) Technique:

Schiedt[14] and Stimson[16] gave the solid sample preparation method for this technique. They assumed that a transparent disc can be made by assimilating properly a suitable matrix material with the sample and by applying a pressure of 1.5×10^4 lbs/inch^2. The matrix material should have comparable with that of refractive index of the sample and should have high transmittance power throughout the spectral range of the instrument alongwith its stability and nonhygroscopicity. Normally, the matrix materials used are the alkalihalides like KBr, KCl, NaCl, KI etc. KBr is more widely used in this method.

REFERENCES

1. Gesi K., Phys. Status Solidi **a33** 391 (1976).
2. Operational Manual of Spectra Physics (165).
3. Operation and Maintenance Instruction Manual for Spex Model 1403 Spectrometer (1982).
4. Turrell G. "Infrared and Raman Spectroscopy" Academic Press, London (1972).
5. Porto S.P.S. in "Light Scattering with Laser Sources in Light Scattering Spectra of Solids" ed. by G.B. Wright, Springer-Verlag, Berlin (1969).
   Damen T.C., Porto. S.P.S. and Tell B., Phys. Rev. **144** 771 (1966).
6. Loader J. "Basic Laser Raman Spectroscopy" Heyden and Son Ltd.
7. Kendall D.N. "Applied IR Spectroscopy", Reinhold Publishing Corp. New York (1965).
8. Harrick N.J. "Internal Reflection Spectroscopy" John Willey & Sons, INC., New York (1970).
9. Hossain M.A. "M.Phil. dissertation", Dept. of Physics, A.M.U., Aligarh, India (1990).
10. Fahrenfort J., Spectrochim Acta. **17** 698 (1961).
11. Fahrenfort J., and Visser V.M., Spectrochim Acta **48** 1103 (1963).
12. Barnes R.B. Gore R.C., Liddel V. and Van William Z. "IR Spectroscopy" Reinhold, New York (1944).
13. Price W.C. and Tetlom K.S., J. Chem. Phys. **16** 1157 (1948).
14. Schiedt U. and Reinwein H., Z. Naturforsch **7** 270 (1952).
15. Rao C.N.R. "Chemical Application of IR Spectroscopy" Academic Press, New York (1963).
16. Stimson M. and O'Donnell M.J., J. Amer. Chem. Soc. **14** 1805 (1952).

CHAPTER - III

VIBRATIONAL SPECTRA AND PHASE TRANSITION

VIBRATIONAL SPECTRA AND PHASE TRANSITION

3.1 INTRODUCTION

Vibrational spectroscopic methods have been used over the past several years to investigate the molecular dynamics of SPTs and related phenomena. A direct study of molecular vibrational excitations or phonons and their anharmonic interactions and coupling to relaxational and electronic excitations can be carried out using these methods[1]. Nowadays, the techniques of IR and Raman spectroscopy are being extensively employed for the study of effects on normal modes of vibrations in crystals which undergo phase transitions. These two measurements have the advantage of providing complementary information about the vibrational spectra. This chapter is devoted to the study of a few phase transitions in triammonium hydrogen disulphate $(NH_4)_3H(SO_4)_2$ crystal using these experimental methods.

Triammonium hydrogen disulphate $(NH_4)_3H(SO_4)_2$ (hereafter referred to as TAHS) has acquired special importance because of its very strong and unusual O-H···O hydrogen bonds linking SO_4^{2-} ions into a $(SO_4HSO_4)^{3-}$ dimer[2] and its numerous successive phase transitions[3-6]. It has six polymorphic modifications at normal pressure:

Phase I $\left(\begin{matrix}\text{Trigonal}\\ R\bar{3}m\end{matrix}\right)$ $\xrightarrow{413K}$ Phase II $\left(\begin{matrix}\text{Monoclinic}\\ A2/a\end{matrix}\right)$ $\xrightarrow{265K}$

Phase III (Monoclinic) $\xrightarrow{140K}$ Phase IV $\xrightarrow{133K}$ Phase V

$\xrightarrow{46K}$ Phase VI (Ferroelectric).

The application of pressure and deuterium substitution also stabilize the ferroelectric phase of the crystal[7-9]. The pressure induced phase below liquid nitrogen temperature is same as the phase below 46K at atmospheric pressure[10].

The phase I is trigonal with the space group $R\bar{3}m$ or $R\bar{3}c$ and the lattice parameters are a_t = 8.29 A° and α_t = 41.7°[11]. The room temperature phase, Phase II, has monoclinic symmetry with space group A2/a[12]. Later, it was reported that it belongs to the space group C2/c[13]. But, most of the isostructural crystals belong to the space group A2/a[14]. In phase II, the crystal is biaxial and becomes uniaxial in phase I[3,4]. It also shows the ferroelasticity in room temperature phase[15]. From EPR results, Minge and Waplak[16] suggested that the phase transitions II —> III, III —> IV and IV —> V take place within monoclinic symmetry. In phase III, it shows the antiferroelectricity[17] and has an incommensurate structure[18]. The phase transitions I—>II, IV—>V,

V—>VI are found to be of first order in nature whereas the transitions II—>III and III—>IV show second order behaviour[5,6,11].

The work done earlier on TAHS is as follows:

Gossner[3] and Fischer[4] carried out the optical measurements and found out the uniaxial properties in phase I. Pepinsky et al[15] and later Gesi[5,6] have made a detailed dielectric study and showed that there exist in total six phases. Gesi also carried out the differential thermal analysis in detail. The dc electrical conductivity, differential thermal analysis and coulometric studies have been done by Reddy et al[19] at temperatures above room temperature and the transition at 413K confirmed. They showed that the charge carriers in this crystal are protons. They also studied the thermally stimulated depolarization current[20]. The effect of impurity on conductivity has been studied by doping divalent cations by Syamaprasad and Vallabhan[21]. In the temperature range from 100 to 450K, the linear thermal expansion was measured using x-ray diffractometer and dilatometer by Suzuki[11]. He observed a large anisotropy in the linear thermal expansion coefficient along the pseudo-orthorhombic axes. The effect of pressure and deuterium substitution has been studied by Gesi and Osaka et al[8-10]. Suzuki and Makita[12] and Leclaire et al[13] gave the details of crystal structure in the room

temperature phase. The specific heat has been measured above the liquid nitrogen temperature by Suzuki et al[18]. They estimated the entropy at around transition points for phases above 90K. The NMR study has been done by Walton and Reynhardt[22] where they discussed the motion of NH_4 ions. The phase transitions studies above 90K employing EPR technique have been made by Fujimato and Sinha[23], Minge and Waplak[16] and Babu et al[24] using different EPR probes. The IR spectra of powdered samples in three phases have been studied by Acharya and Narayanan[25]. IR and Raman spectra have been investigated below room temperature by Damak et al[2] and Kamoun et al[26] in powder samples. Damak et al assigned the band frequencies for the phase II and V. They concluded that the room temperature phase is strongly disordered because of an orientational disorder of ammonium ions and ordering takes place with the lowering of temperature. Kamoun et al discussed hydrogen bonding, the nature and degree of structural (dis) order and the mechanisms of the phase transitions. They concluded that NH_4 ions are involved in all transitions and their motion seems to be the main cause for the occurrence of ferro-electricity. They have also given the assignment of bands in the internal and external modes regions in different phases. IR and polarized Raman spectra of TAHS have been studied at room temperature by Rajagopal and Aruldhas[27]. They concluded that

NH_4^+ ion is not rotating freely in the lattice. Srivastava et al[28] have studied the far-IR reflectivity and polarized Raman spectra of single crystals in the temperature range from 10 to 300K. They showed that the effects of anharmonicity and the ordering of coupled motions of cations and anions cause the ferro-electric transition. They also assigned the bands in different phases. From reflectivity spectra, a reversal of the trend in the shift of longitudinal optical mode frequency has been detected for the transition, phase III ⟶ phase IV. They also suggested the change of site symmetry of NH_4^+ and SO_4^{2-} ions is associated with the transitions, phase III ⟶ phase IV and phase IV ⟶ Phase V.

The dynamics of NH_4^+ and SO_4^{2-} ions plays an important role in phase transitions in TAHS which can be studied by IR and Raman spectroscopy. EPR measurements[24] suggested that the reorientational motion of NH_4^+ and SO_4^{2-} ions is responsible for the transitions pahse III ⟶ phase IV and phase IV ⟶ phase V. But from Raman measurements reported earlier[28], it has been shown that the change of site symmetry of SO_4^{2-} and NH_4^+ ions is associated with phase transitions. There is some doubt that the symmetric stretching mode ν_1 vanishes in phase IV. In the present work we have concentrated on the transitions, phase III $\xrightarrow{140K}$ phase IV and phase IV $\xrightarrow{133K}$ phase V. We have employed

Raman spectroscopic method for this study. We have taken the polarized Raman spectra at different temperatures in the vicinity of the transitions over the frequency range 900-1250 cm^{-1} to understand the role of sulphate ions in these transitions. For assignments of the bands we have also taken the IR spectra for powdered samples at room temperature.

3.2 CRYSTAL STRUCTURE:

TAHS crystalizes as single domain within the monoclinic symmetry at room temperature. It has four formula units per unit cell. The space group is A2/a[12] in this phase. The unit cell parameters are a = 10.153 A°, b = 5.854 A°, c = 15.410 A°, $\alpha = \beta = 90°$ and $\gamma = 101.76°$[12]. Suzuki and Makita[12] have determined the structure at room temperature. They determined the positions of S and O atoms from **'three dimensional Patterson synthesis'** and positions of N atoms from **'block-diagonal least squares refinements'.** The crystal structure is shown in Fig. 3.1.

There are twelve ammonium ions and eight sulphate ions in a unit cell. Each pair of neighbouring sulphate ions linked by one hydrogen bond of the type O-H··· O forms a $(SO_4HSO_4)^{3-}$ dimer. The sulphate ions contain four hydrogen bonds of this type.

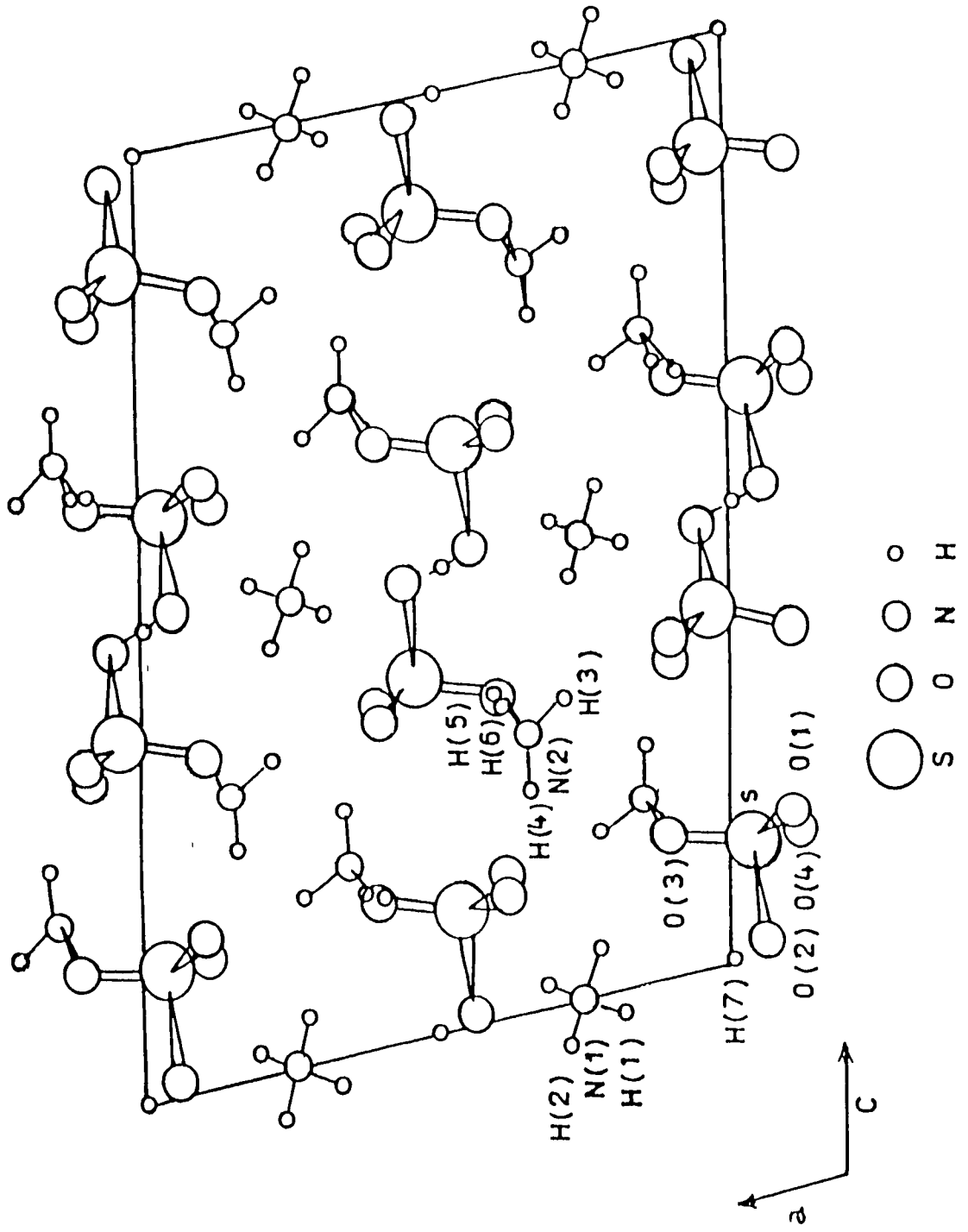

Fig. 3.1. Crystal Structure of TAHS Projected along b-axis for Phase II.

There also exists N-H··· O type hydrogen bonding. Ammonium ions occupy two sets of non-equivalent positions: one set at general positions, NH_4^+ (2) and other at special positions on two-fold axis, NH_4^+(1). There are four NH_4^+ (1) ions and eight NH_4^+ (2) ions in the unit cell. Each H atom bonded to N(1) atom forms a N-H···O type hydrogen bond and the one bonded to N(2) forms N-H···20 type bifurcated bond. NH_4^+ (1) ions form slightly distorted tetrahedra having electric dipole moment and are statistically ordered[12]. The sulphate ions carry an electric dipole moment parallel to the S-O(2)[12] bond whose bond length is different from other S-O bonds. Thus, sulphate ions are also slightly distorted.

3.3 FACTOR GROUP ANALYSIS:

The factor group C_{2h} has the symmetry species A_g, B_g, A_u and B_u. The vibrations belonging to A_g and B_g show Raman activity whereas A_u and B_u symmetric vibrations are IR active. Vibrations of A_g symmetry are permitted in XX, YY, ZZ and XZ polarizations and those of B_g symmetry in XY and YZ only. When electric vector of the incident radiation is parallel to Y-axis, then A_u symmetry modes appear in the IR spectrum. The B_u symmetry modes are expected to appear when the electric vector of the incident IR beam is made parallel to either X or Z-axis.

We have classified the normal modes of vibrations by using correlation method after Fateley et al[29]. Site symmetry at each equivalent set of atoms or ions should be known for this method. There are four equivalent sets of atoms or ions in the crystals. These are four $NH_4^+(1)$ ions eight $NH_4^+(2)$ ions, eights SO_4^{2-} ions and the four hydrogen atoms. The possible site symmetries for the space group C_{2h}^6 are $C_1(8)$, $C_2(4)$ and $4C_i(4)$. As NH_4^+ (1) ions are on two fold axis, site symmetry for these ions will be C_2. The C_i site has the multiplicity four. So four hydrogen atoms can be accommodated at this site. The C_1 site has the multiplicity eight, and it can take infinite numbers in the crystals. Hence $NH_4^+(2)$ and SO_4^{2-} ions will be accommodated at C_1 sites. Thus the site symmetry for different site of ions or atoms are

$NH_4^+(1)$	----------	$C_2(4)$
$NH_4^+(2)$	----------	$C_1(8)$
SO_4^{2-}	----------	$C_1(8)$
H	----------	$C_i(4)$

The total number of modes are 312, including 3 acoustic modes. From group theoretical analysis we have shown that there are 108 internal modes of NH_4 ions, 72 internal modes of SO_4^{2-} ions and 132 external modes in the crystals. The external modes include 60 libratory modes and 72 translatory modes.

TABLE 3.1 - Correlation between different species free state groups, site groups and factor group of different atoms and ions in TAHS.

Structural group	Symmetry species		
	Free State	Site group	Factor group
$NH_4^+(1)$	T_d	C_2	C_{2h}
	A_1	A	A_g
	A_2		B_g
	E		A_u
	F_1	B	B_u
	F_2		
$NH_4^+(2)$ & SO_4^{2-}	T_d	C_1	C_{2h}
	A_1	A	A_g
	A_2		b_g
	E		A_u
	F_1		B_u
	F_2		
H^+		C_i	C_{2h}
		A_g	A_g
			B_g
		A_u	A_u
			B_u

TABLE 3.2 - Classification of phonons in TAHS crystal at room temperature phase.

Modes	Species under C_{2h}				Total number of phonon modes for particular mode of vibration.
	A_g	B_g	A_u	B_u	
1. Internal modes of NH_4^+ (1):					
$\nu_1(A_1)$	2	0	2	0	4
$\nu_2(E)$	4	0	4	0	8
$\nu_3(F_2)$	2	4	2	4	12
$\nu_4(F_2)$	2	4	2	4	12
Total internal modes	10	8	10	8	36
Internal modes of NH_4^+(2)					
$\nu_1(A_1)$	2	2	2	2	8
$\nu_2(E)$	4	4	4	4	16
$\nu_3(F_2)$	6	6	6	6	24
$\nu_4(F_2)$	6	6	6	6	24
Total internal modes	18	18	18	18	72
Total number of modes of NH_4^+ ions	28	26	28	26	108

Contd.... (Table 3.2)

Modes		Species under C_{2h}				Total number of phonon modes for particular mode of vibration.
		A_g	B_g	A_u	B_u	
(ii)	Internal modes of SO_4^{2-} ions					
	$\nu_1(A_1)$	2	2	2	2	8
	$\nu_2(E)$	4	4	4	4	16
	$\nu_3(F_2)$	6	6	6	6	24
	$\nu_4(F_2)$	6	6	6	6	24
	Total internal modes of SO_4^{2-} ions	18	18	18	18	72
(iii)	External modes:					
(a)	Libratory modes of $NH_4^+(1)$	2	4	2	4	12
(b)	Libratory modes of $NH_4^+(2)$	6	6	6	6	24
(c)	Libratory modes of SO_4^{2-}	6	6	6	6	24
(d)	Translatory modes of $NH_4^+(1)$	2	4	2	4	12
(e)	Translatory modes of $NH_4^+(2)$	6	6	6	6	24
(f)	Translatory modes of SO_4^{2-}	6	6	6	6	24
(g)	Translatory modes of H^+	0	0	6	6	12
	Total external modes	28	32	34	38	132
	Total number of modes in the crystal	74	76	80	82	312

The **correlation** between the different symmetry species of free state point group, site symmetry point group of atoms and ions in the crystal and the crystal factor group are given in the table 3.1. Using this **correlation chart** of the symmetry species, the number of the phonon modes arising from definite mode of free state ammonium and sulphate ions along with the translatory and libratory modes and the translatory modes of H- atom are listed in table 3.2.

3.4 RESULTS AND DISCUSSIONS:

3.4.1 Vibrational spectra and bands assignment at room temperature:

The polarized Raman spectra of TAHS have been taken in the frequency range 40-3250 cm^{-1} at room temperature and is shown in Fig. 3.2. The laboratory orthogonal system of coordinate X Y Z is related to the crystallographic axes a, b of monoclinic symmetry of the crystal as X//a, Y//b and Z//axb. IR absorption spectra for microcrystalline samples have also been taken in the frequency range 200-4000 cm^{-1} to help the identification of normal modes. The IR spectrum observed at room temperature is shown in Fig. 3.3. The bands assignment are made by comparing spectra with those observed by previous workers[2, 25-28]. The vibrational modes are identified as internal modes of NH_4^+ , SO_4^{2-} ions and

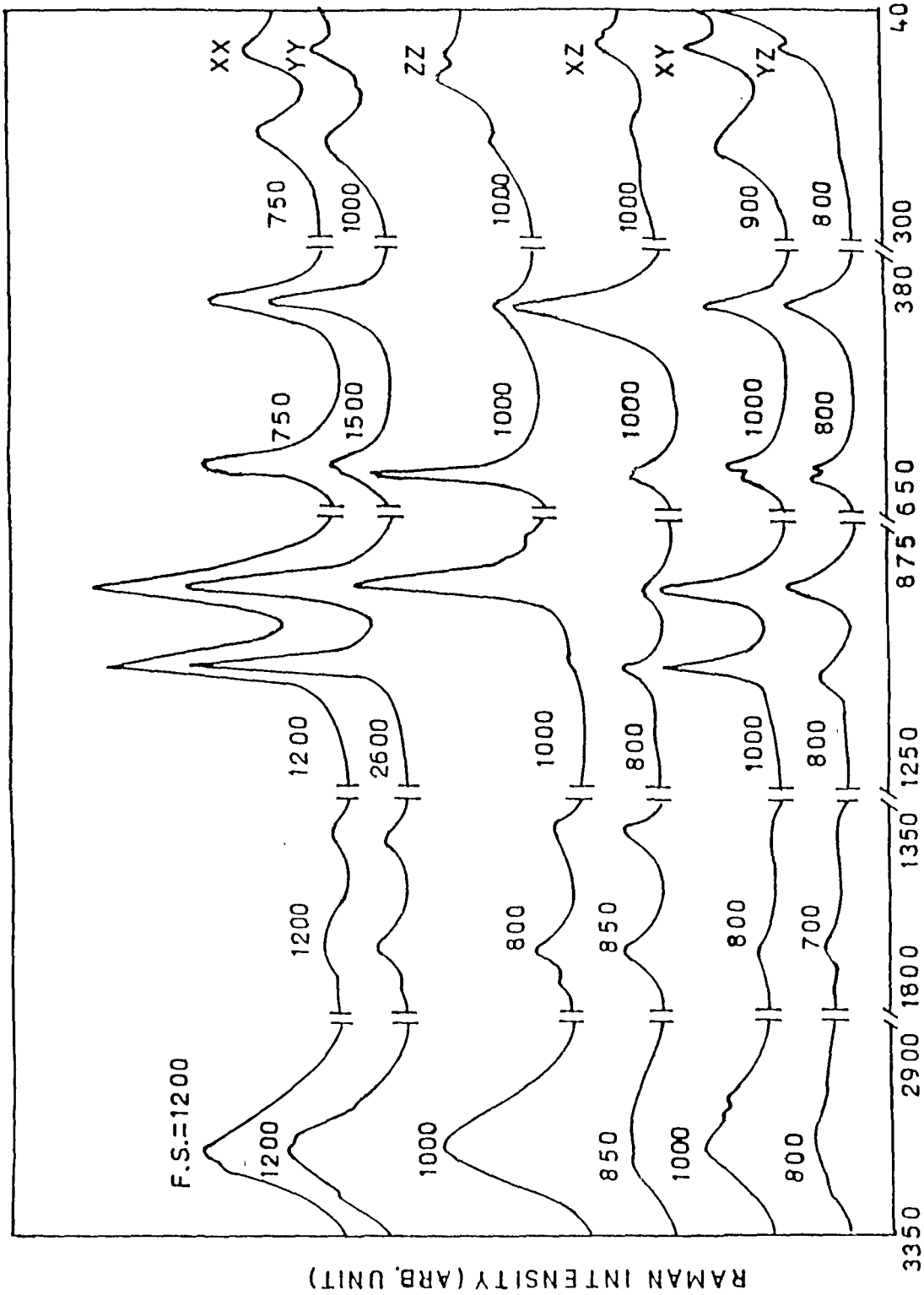

Fig. 3.2. Polarized Raman Spectra of TAHS at room temperature (40-3250 cm^{-1}).

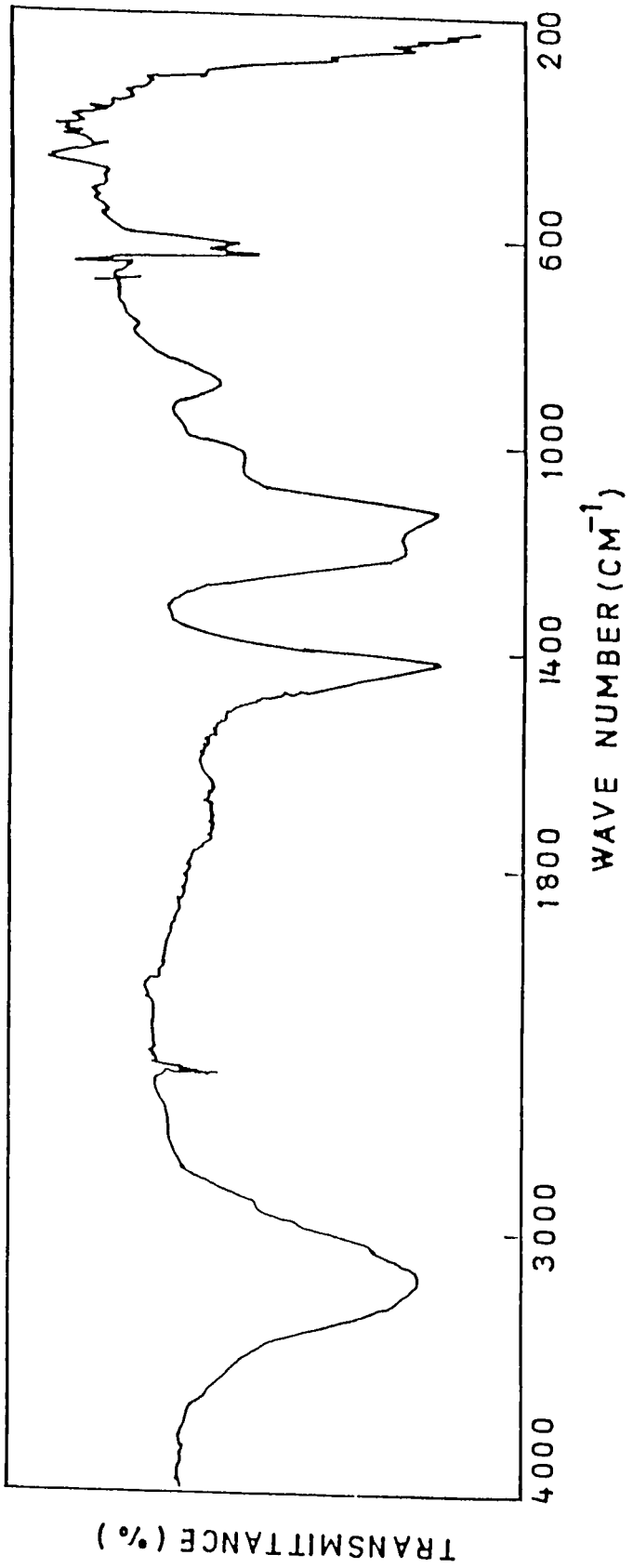

Fig. 3.3. Infrared spectra of TAHS at room temperature (200-4000 cm^{-1}).

lattice modes. Superscript 'N' and 'S' are used to distinguish the modes of NH_4^+ and SO_4^{2-} ions. The frequencies of observed bands and their assignment are given in table 3.3.

(a) **Internal modes of SO_4^{2-} ion:**

As discussed earlier, there are four fundamental internal modes of vibrations of SO_4^{2-} ion. ν_1^S (A_1) represents nondegenerate totally symmetric S-O stretching and $\nu_3^S(F_2)$ is the triply degenerate asymmetric S-O stretching mode, ν_2^S (E) and $\nu_4^S(F_2)$ are the symmetric and asymmetric O-S-O bending modes respectively. The ν_1 modes of SO_4^{2-} is expected to be very strong and is observed around 980 cm^{-1}[27]. As a result of strong hydrogen bonding, SO_4^{2-} and HSO_4^- are likely to coexist in the crystal with the vibrational interaction between them[2]. Two bands observed around 968 and 1075 cm^{-1} are very strong in XX, YY and ZZ geometries, assigned as totally symmetric stretching vibration ν_1^S. The large separation of these two bands signifies that H-atom is strongly bonded to one of the SO_4^{2-} ions. So, the two stretching modes may be considered for the SO_4^{2-} and HSO_4^- ions. The lower one belongs to HSO_4^- ion.

The presence of HSO_4^- ion in the crystal requires the assignment of internal modes of HSO_4^- [30,31]. The HSO_4^- ion

Table 3.3 : Raman frequencies in different polarization, IR frequencies at room temperature for $(NH_4)_3H(SO_4)_2$ and their assignment. (frequency in cm^{-1} unit).

Raman						IR	Assignment
XX	YY	ZZ	XY	YZ	XZ		
72w				72w	72w		L^S
	84w	85w	82m	82vw	82w		
	120vw	120vw					
186w	191wb	184vwb	191mb	198vwb	186vwb	218w	t^N
						272w	l^N
	409vw					405w	$\gamma_{S\text{-}OH}$
442m	440s	441m	444m	438m	439s	441m	ν_2^S
	458wsh	463wsh	458wsh		459wsh		
		904w	907vw			876m	γ_{OH}
967s	967vs	968vs	967m	967w	969wb	996vw	$\nu_1^S(HSO_4^-)$
						1023w	
1074s	1076vs	1070m	1076m	1075m	1075w		$\nu_1^S(SO_4^{2-})$
			1114vwb	1112vwb	1123vwb	1116s	ν_3^S
						1191m	δ_{OH}

Table Contd...

Table 3.3. Contd...

						1318w	ν_4^N
						1346w	
		1408vw	1416vw		1413m	1403s	
1445vwb	1450wb		1461vw				
1695w	1677wb	1686w	1693vw	1664w	1675mb	1663w	ν_2^N
	1750vw	1750w					$\nu_4^N + l^N$
						2850w	$2\ \nu_4^N$
						2920w	
2998vwb	3073vwb	3000vwb				3020wsh	ν_{OH}
3160wsh	3168s	3160sb	3164wb	3161m	3160wb	3137s	ν_3^N
3223s	3259wsh		3221wsh		3223vw		ν_1^N

vs = very strong, s = strong, m = medium, w = weak, vw = very weak, b = broad, sh = shoulder, L^S = lattice mode of SO_4^{2-} ion, t^N = translatory mode for NH_4^+ ion, l^N = libratory mode for NH_4^+ ion.

is treated as distorted tetrahedral SO_4^{2-} ion. There are twelve modes, nine of which are undistorted SO_4^{2-} ion modes $\nu_1{}^s(A_1)$, $\nu_2{}^s(E)$, $\nu_3{}^s(F_2)$ and $\nu_4{}^s(F_2)$. The remaining three are due to the motion of the hydrogen atom, denoted as ν_{OH} (O-H stretching), δ_{OH} (O-H bending) and γ_{OH} (O-H torsion). These bands are assigned by comparing the present spectra with those of other hydrogen bonded systems[31,32]. The very weak bands at 896 and 3006 cm^{-1} are identified as γ_{OH} and ν_{OH} respectively. The band observed at 1191 cm^{-1} in the IR spectrum is identified with δ_{OH} mode.

The frequency components of $\nu_2{}^s$ and $\nu_4{}^s$ modes of HSO_4^- ion are expected in the corresponding mode frequency region of SO_4^{2-} and they have lower frequencies. $\nu_3{}^s$ mode of this ion can not be separated out from SO_4^{2-} mode because the frequencies of the both ions are mixed around 1120 cm^{-1}. The strong band at 441 cm^{-1} with a shoulder at 460 cm^{-1} is assigned to $\nu_2{}^s$ mode. The asymmetric bending modes $\nu_4{}^s$ are observed as strong bands around 610 cm^{-1}.

(b) **Internal modes of NH_4^+ ions:**

The four internal modes of NH_4^+ ions are denoted as $\nu_1{}^N(A_1)$, $\nu_2{}^N(E)$, $\nu_3{}^N(F_2)$ and $\nu_4{}^N(F_2)$, similar to those for

SO_4^{2-} ion. Here the superscript N is used to denote the NH_4^- ion. A strong broad band is observed with a few components in the N-H stretching region (ν_1^N) in the IR and Raman spectra. It happened so, because of the varying N-H···O bond lengths. The strong peak at 3223 cm^{-1} is assigned to ν_1^N mode. The frequency around 3160 cm^{-1} observed both in the IR and Raman spectra is identified as ν_3^N mode. The weak band around 1685 cm^{-1} is assigned to ν_2^N mode whereas bands in the range 1318 - 1461 cm^{-1} are assigned to ν_4^N. The weak bands around 2900 cm^{-1} and at 1750 cm^{-1} are assigned to two phonon and combination modes respectively. The presence of combination modes eliminates the possibility of free rotation of the ammonium ions in the crystal lattice[33].

The broad character of N-H stretching band indicates that there is a disorder orientational motion of NH_4^+ ion. The corresponding hydrogen bond is too weak to broaden the N-H stretching bands because of anharmonicity. The observed nature of the bands also confirm that the NH_4^+ ions behave like perfect tetrahedral ions in the crystal and are ordered in state.

(c) **Lattice modes:**

Clear-cut assignments of low frequency bands in the spectra are not easy but we can work out a general assignment on the

basis of bands observed in the compounds containing either SO_4^{2-} or NH_4^+ ions[34-36]. These assignments have been undertaken on the basis that the translatory and libratory modes of NH_4^+ ions occur at frequencies higher than that of the corresponding modes of SO_4^{2-} ion (mass ratio: NH_4^+ : SO_4^{2-} = 1:5.3) and the vibrational bands due to librational modes will generally be weak[37]. Therefore, the lowest frequencies below 150 cm^{-1} are considered as lattice modes for SO_4^{2-} ion. The next lowest frequencies (150-250 cm^{-1}) are attributed to the translatory modes of NH_4^+ ions whereas in the range 250-350 cm^{-1} could belong to the libratory mode of NH_4^+ ion.

3.4.2 Temperature dependent Raman spectra and Phase Transition:

We have taken the polarized Raman spectra in XX, XY and XZ geometries at a few selected temperatures in the range from room temperature to 125K. We have got the same type of change in XX polarization as observed by Kamoun et al[26]. There were no significant changes in XY geometry except the downward frequency shift in the N-H stretching mode region. But according to earlier work[28] in XY geometry the symmetric stretching mode ν_1 vanishes in phase IV. Thus our findings in XY polarization are not in agreement with this observation. We have noticed more thermosensitive bands in XZ geometry, shown in Fig. 3.4. We have

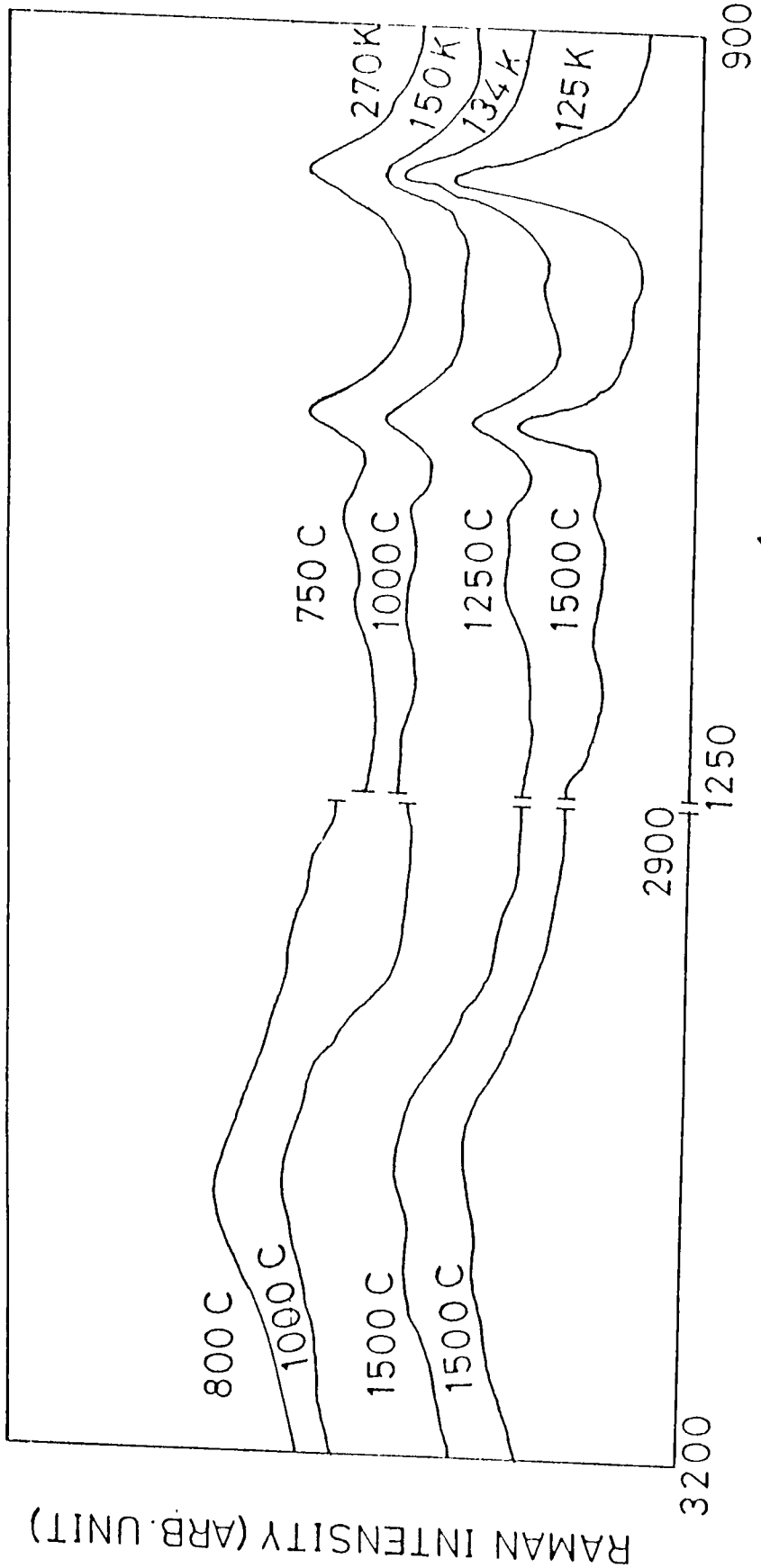

Fig. 3.4: Temperature dependence of Raman spectra in XZ geometry.

observed the downward shift of N-H stretching modes and the variation of peak intensity and full width at half maximum (FWHM) of the HSO_4^- symmetric stretching mode (968 cm^{-1}) for the phase changes III —> IV and IV —> V. The N-H stretching modes are very weak and broad, so accurate measurements are difficult for these bands. We have recorded temperature dependent spectra in the region of HSO_4^- symmetric stretching mode in the temperature range 160 to 125 K to study the nature of change of 968 cm^{-1} band in these two transitions. The temperature dependent Raman spectra observed in this region are shown in Fig. 3.5. The variation of full width at half maximum and peak intensity as a function of temperature of the band at 968 cm^{-1} are displayed in Fig. 3.6. The important features of temperatue dependence of Raman spectra of the system are as follows:

(1) The peak intensity of 968 cm^{-1} band assigned as HSO_4^- symmetric stretching mode is almost same with the temperature decreasing till 142K. With further decrease in temperature, the peak intensity increases continuously upto 134K. If we reduce the temperature further, then around 133K, a drastic increase in peak intensity occurs. Below 132 K, the peak intensity increases linearly without any remarkable change.

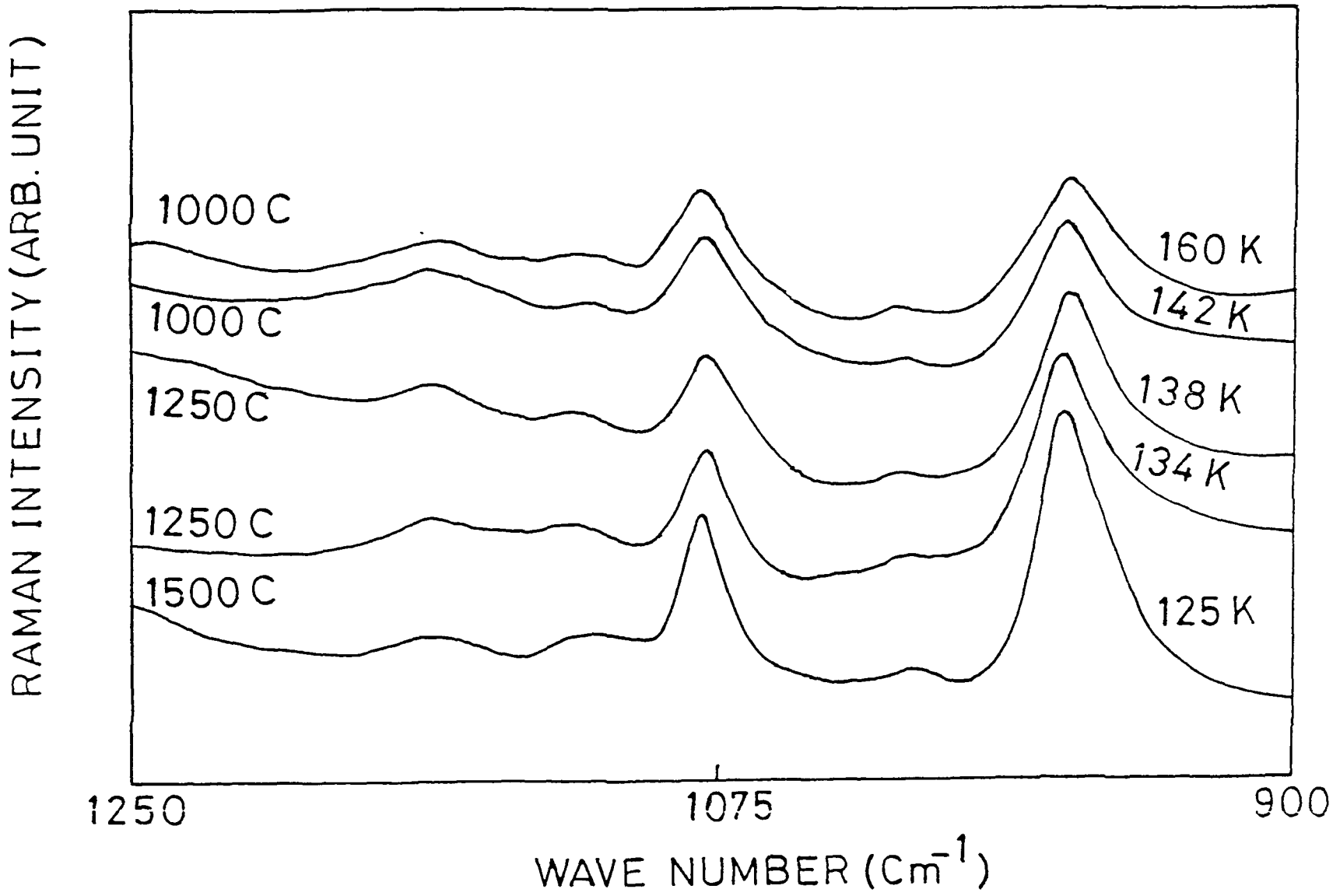

100

Fig. 3.5. Temperature dependent Raman Spectra in the frequency range 900-1250 cm^{-1} in XZ geometry.

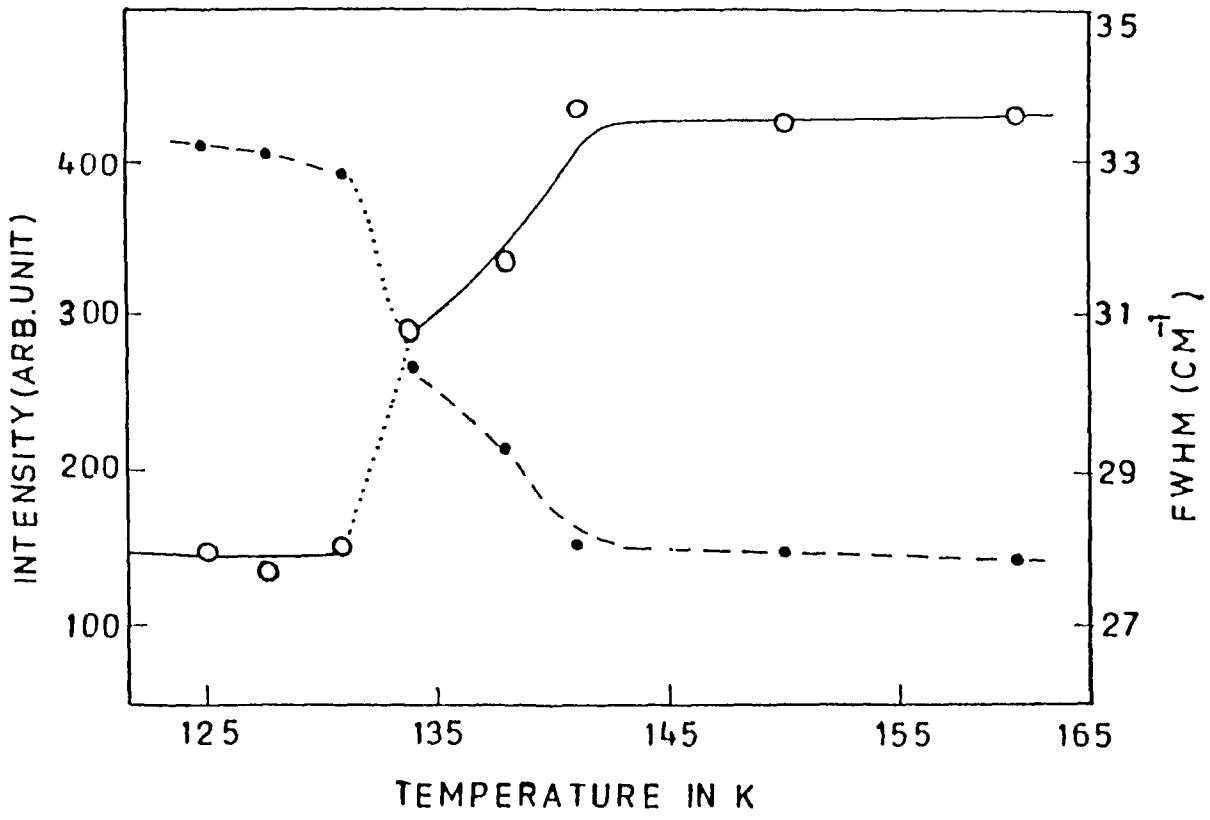

Fig. 3.6. Variation in Peak Frequency and full width at half maximum with temperature of the HSO_4^- symmetric stretching mode in XZ geometry.

(2) The full width at half maximum (FWHM) of the band associated with the HSO_4^- symmetric stretching mode at 968 cm^{-1} remains nearly constant as the temperature drops to 142K. When the temperature decreases further below 142K, the FWHM decreases continuously in a well defined manner till 134K. There is an abrupt decrease in FWHM around 133K and then keeps almost constant with the further reduction of temperature.

As the temperature decreases, the peak intensity of the HSO_4^- symmetric stretching mode increases continuously with a linearly decreasing FWHM around 140K. It is an evidence of the second order phase transition whereas, the sudden increment of peak intensity of HSO_4^- symmetric stretching mode around 133K with abrupt decrease of FWHM confirms that there is a first order phase transition around 133K. Thus the transition III⟶IV and IV⟶V are second order and first order type respectively which is consistent with the findings of earlier worker[11].

From temperature dependent feature of peak intensity and FWHM, one can calculate the value of order-parameter and activation energy of reorientational motion of the ions. Here the two phases are in narrower temperature range, so it is difficult to

get the sufficient data to calculate the value of order-parameter and activation energy. It also depends on the accuracy of the instruments. However, following the approach of earlier workers[38,39], we can explain our findings as follows:

The width of bands arises essentially due to the interruption of the vibrations by various physical processes. In a disordered crystals, there are various rotational motion of the molecule of the crystals and have multiple orientational sites. For equivalent sites the band shape is given as a result of overlap of Lorentzion functions which are located at the same central position but have different widths[38]. The line width of a band is also expected to decrease due to the freezing of the disorientations into finite directions[39]. We have seen that the HSO_4^- symmetric stretching mode of 968 cm^{-1} is narrower in FWHM without any change in frequency. The peak intensity also increases with the temperature lowering and the band shape retained as Lorentzion. Thus we can conclude that the orientational motions of HSO_4^- ions within the same site position, which is not in agreement with the previous workers[28]. The decrease of N-H stretching mode frequency indicates that the hydrogen bonding are increases in NH_4^+ ions as the temperature decreases and also causes the reorientation of NH_4^+ ions. Thus the reorientation motion of both the molecular

ions are mutually effective in the phase transition III—>IV and IV—>V. The temperature dependence behaviour of both the ions revealed that both the ions reorient to retain on effective tetrahedral symmetry in the lattice.

3.5 CONCLUSIONS

(i) The transitions around 140K and 133K are of the second order and first order in nature respectively.

(ii) The reorientational motion of both NH_4^+ and SO_4^{2-} ions take place during these transitions without changing their site symmetry.

REFERENCES

1. Iqbal Z. In "Vibrational Spectroscopy of Phase Transitions" ed. Zafar Iqbal and F.J. Owens, Academic Press INC (1984).
2. Damak M., Kamoun M., Daoud A., Romain F., Lautie A. and Novak A., J. Mol. Struc. **130** 245 (1985).
3. Gossner B., Z. Kristallogr **38** 110 (1904).
4. Fischer P., Z. Kristallogr **54** 528 (1914).
5. Gesi K., J. Phys. Soc. Japan **41** 1437 (1976).
6. Gesi K., Jpn. J. Appl. Phys. **19** 1051 (1980).
7. Gesi. K., Phys. Status Solidi **a33** 479 (1976).
8. Gesi K., J. Phys. Soc. Japan **43** 1941 (1977).
9. Osaka T., Makita Y. and Gesi K., J. Phys. Soc. Japan, **43** 933 (1977).
10. Osaka T., Makita Y. and Gesi K., J. Phys. Soc. Japan **49** 593 (1980).
11. Suzuki S., J. Phys. Soc. Japan **47** 1205 (1979).
12. Suzuki S. and Makita Y., Acta. Cryst. **B34** 732 (1978).
13. Leclaire P.A., Ledesert M., Monier C.J., Daoud A. and Damak M., Acta Crystallogr. Sect **B41** 209 (1985).
14. Noda Y., Kasatani H., Watanabe Y., Teranchi H. and Gesi K., J. Phys. Soc. Japan **59** 3249 (1990).
15. Gesi K., J. Phys. Soc. Japan **41** 1437 (1976).
16. Minge J. and Waplak S., Phys. Status Solidi **b123** 27 (1984).
17. Pepinsky R., Vedam K., Hoshino S. Makita Y., Phys. Rev. **111** 1508 (1958).
18. Suzuki S., Takahashi M., Makita Y. and Gesi K. "Presented at the meeting of physical society of Japan" Yamagata (1976).
19. Reddy A.D., Sathyanarayan S.G. and Sastry G.S., Solid state commun. **43** 937 (1982).

20. Reddy A.D., Sathyanarayan S.G. and Sastry G.S., Phys. Status salidi **a79** 575 (1983).
21. Syamaprasad U. and Vallabhan C.P.G., J. Phys. C: Solid State Phys. **14** 571 (1981).
22. Walton A. and Reynhardt E.C., J. Chem. Phys. **65** 4370 (1975).
23. Fujimato M. and Sinha B.V., Ferroelectrics **46** 227 (1983).
24. Babu D.S., Sastry G.S., Sastry M.D. and Dalvi A.G.I., J. Phys. C: Solid State Phys. **18** 6111 (1985).
25. Acharya P.K. and Narayanan P.S., Ind. J. Pure and Appl. Phys. **11** 574 (1973).
26. Kamoun M., Lautie A., Romain F. and Novak A., J. Raman Spectrosc. **19** 329 (1988).
27. Rajagopal P. and Aruldhas G., J. Raman Spectrosc. **19** 497 (1988).
28. Srivastava J.P., Kulshreshtha A., Kullmann W. and Rauh H., J. Phys. C: Solid State Phys. **21** 4669 (1988).
29. Fateley W.G., Dollish F.R., McDavitt N.T. and Bentley F.F. "Infrared and Raman Selection Rules for Molecular and Lattice Vibrations: correlation method" Wiley-Interscience, New York (1972).
30. Kulshreshtha A. "Ph.D. Thesis" Dept. of Phys., A.M.U., India (1988).
31. Schutte C.J.H. and Van Rensburg D. J.J., J. Mol. Struc. **9** 77 (1971).
32. Baron J., J. Mol. Struc. **162** 211 (1987).
33. Oxton I.A. and Knop O., Can. J. Chem. **57** 404 (1979).
34. Torrie B.H., Lin C.C., Binbrek O.S. and Anderson A., J. Phys. Chem. Solids **33** 697 (1972).
35. Gupta S.P. "Ph.D. Thesis" A.M.U., Aligarh, India (1984).
36. Chakraborty T. and Verma A.L., Phys. Rev. B **39** 3835 (1989).

37. Venkaleswarlu P., Bist H.D. and Jain Y.S., J. Raman Spectrosc. **3** 143 (1975).

38. Yonghae Cho, Masamichi Kobayashi and Hiroynki Tadokoro, J. Chem. Phys. **84** 4643 (1986).

39. Rathore R.P., Khatri S.S. and Chakraborty T., J. Raman Spectrosc. **18** 429 (1987).